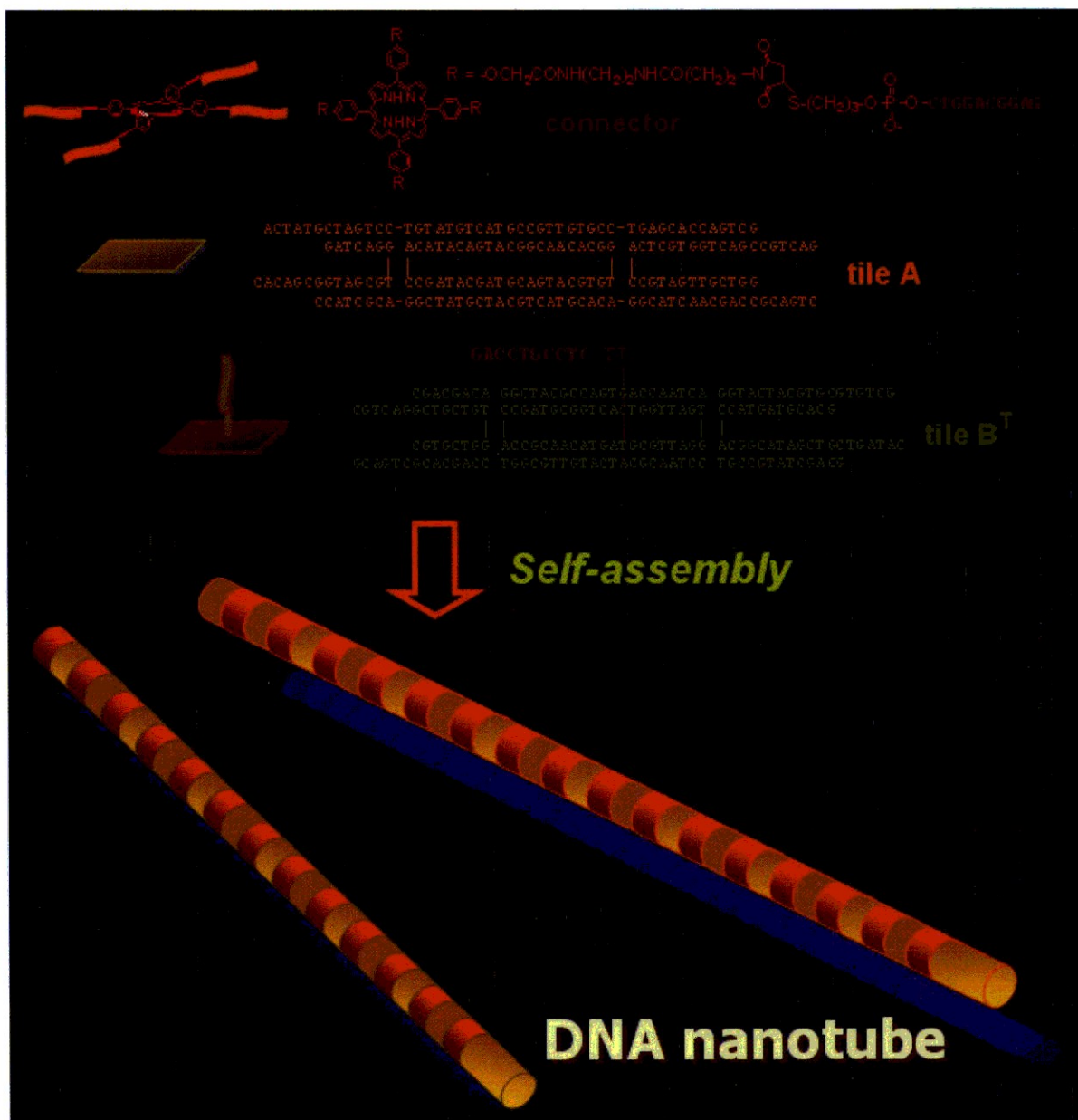


# Soft NANOMATERIALS



## CHAPTER 3

# Polypeptide Multilayer Films and Microcapsules

**Bingyun Li**

*Department of Orthopedics, School of Medicine and WVNano Initiative, West Virginia University,  
Morgantown, WV 26506, USA*

### CONTENTS

1. Introduction	1
2. Polypeptide and Polypeptide Synthesis	3
2.1. Polypeptide—An Innovative Biomaterial	3
2.2. Chemical Synthesis of Polypeptides	4
3. Techniques for Fabrication of Polypeptide Multilayers	5
3.1. Langmuir-Blodgett (LB) Technique	5
3.2. Electrostatic Layer-by-Layer (LBL) Self-Assembly	6
4. Techniques for Monitoring and Characterizing Polypeptide Multilayer Formation	7
4.1. Quartz Crystal Microbalance (QCM)	7
4.2. UV-Vis	7
4.3. Atomic Force Microscopy (AFM)	8
4.4. Fluorescence Microscopy	8
4.5. Ellipsometry	8
4.6. Fourier Transform Infrared Spectroscopy (FTIR)	9
4.7. Circular Dichroism (CD) Spectroscopy	9
5. Polypeptide Multilayer Films and Microcapsules	9
5.1. Polypeptide Multilayer Films Prepared Using LB Technique	9
5.2. LBL Multilayers of Poly(L-lysine)/Poly(L-glutamic acid)	10
5.3. LBL Multilayers of Designed Polypeptides	14
5.4. Multilayers Consisting of One Polypeptide and One Non-Polypeptide Component	22
5.5. Polypeptide Microcapsules	22
6. Applications of Polypeptide Multilayers	23
6.1. Chiral Separation	23
6.2. Anti-Inflammatory Coatings	24
6.3. Polypeptide Multilayers as Electrochemical Interfaces for Ion and Electron Transport	25
6.4. Polypeptide Multilayers in Nanofiltration for Ion Separation	25
7. Conclusions and Future Prospects	25
References	26

ISBN: 1-58883-133-7  
Copyright © 2009 American Scientific Publishers  
All rights of reproduction in any form reserved.

*Soft Nanomaterials*  
Edited by Hari Singh Nalwa  
Volume 2: Pages (123-150)

## 1. INTRODUCTION

In recent years, polypeptide multilayers, including multilayer films and microcapsules, have attracted considerable attention due mainly to the close relationship of polypeptides to native biological molecules and the ordered secondary structures ( $\alpha$ -helix and  $\beta$ -sheet) of polypeptides and polypeptide multilayers. For instance, the interaction of oppositely charged 32-mer polypeptides leads to multilayer films presenting a predominantly  $\beta$ -sheet content [1, 2] and poly(L-lysine)/poly(L-glutamic acid), i.e., PLL/PLGA films, a high  $\alpha$ -helix content [3]. The ordered secondary structures are useful in creating self-organized functional surfaces [4, 5], and their biological nature makes polypeptides useful for numerous applications requiring biocompatible interfaces [6]. Moreover, by designing suitable primary (and secondary) structures, polypeptides and polypeptide multilayers can be endowed with specific biofunctionalities. The number of possible, and, indeed, realizable polypeptide sequences is effectively unlimited; this provides flexibility in polypeptide design and the polypeptide multilayer design process.

Polypeptide multilayers are the subject of fundamental structural studies [7–9] for biomedical and pharmaceutical applications [10–13] and for biomimetic surface modifications [1–3]. Different approaches have been taken in polypeptide multilayer formation. Two well-known techniques are Langmuir-Blodgett (LB) deposition and electrostatic layer-by-layer self-assembly (LBL). The latter, first proposed by Iler [14] and extended by Decher [15], provides a simple, versatile, environmentally efficient method of preparing polypeptide multilayers on the nanometer scale [1, 16].

Polypeptides and proteins are natural polymers. Proteins including cytochrome c, lysozyme, histone f3, myoglobin, hemoglobin, pepsin, albumin, immunoglobulin G, peroxidase, glucose oxidase, and catalase have been used for LBL of multilayers. The applications of proteins for LBL and LB multilayers have been reviewed [17–19] and will not be discussed here. Polypeptides are generally less complex than proteins, which may present a number of difficulties for multilayer formation. Direct assembly of oppositely charged protein molecules has been found to be difficult; the preparation of glucose oxidase/lysozyme composite layers has failed [17]. This is probably because electrostatic attraction cannot be maximized with globular proteins in the LBL process.

This chapter provides an overview of polypeptide multilayer films and microcapsules with particular emphasis on multilayers made of designed polypeptides. Multilayers made of commercially available polypeptides such as PLL and PLGA are also discussed in detail. The chemical methods for polypeptide synthesis are described, and the approaches used to form polypeptide multilayer films and microcapsules are outlined. The applications of widely used physical techniques for monitoring polypeptide multilayer formation are briefly reviewed. The applications of polypeptide multilayers are discussed and some examples given.

## 2. POLYPEPTIDE AND POLYPEPTIDE SYNTHESIS

### 2.1. Polypeptide—An Innovative Biomaterial

There are four major types of biological macromolecules; polypeptides are one type. Polypeptides are natural or synthetic linear polymers based on approximately 20 amino acid monomers [Table 1]. They contain an amino group ( $-\text{NH}_2$ ) and a carboxyl group ( $-\text{COOH}$ ) attached to a central carbon atom. However, each amino acid has a different side group attached to the central carbon that lends unique character to that amino acid. The side group can be hydrophobic, hydrophilic, positively charged, or negatively charged at neutral pH [20]. The amino acids are linked covalently by peptide bonds. Scheme 1 shows how four amino acids linked by peptide bonds form a tetrapeptide.

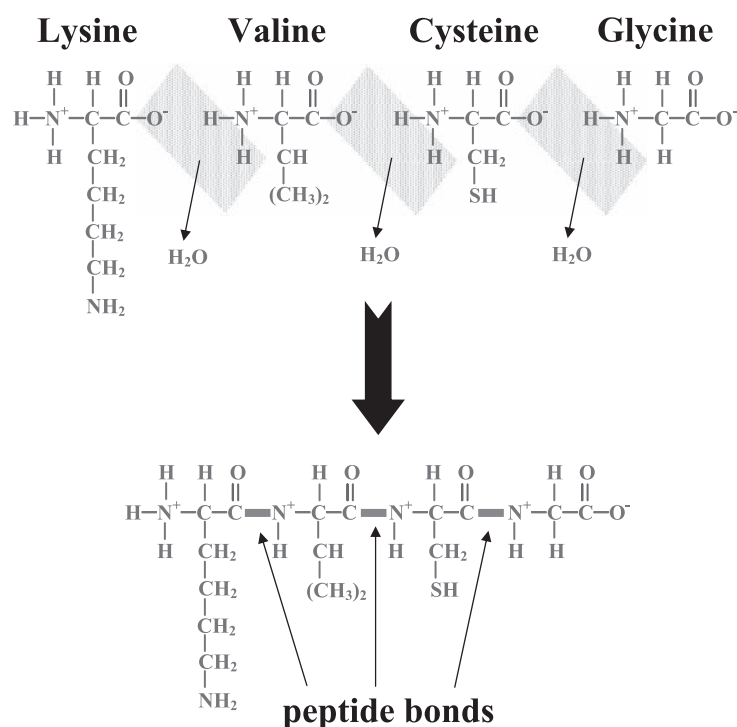
There are four levels of structures found in polypeptides: primary, secondary, tertiary, and quaternary structures. Depending on the sequential order of the amino acids (primary structure of the polypeptide), the polypeptide assumes different structures along the polymer chain (secondary structure of the polypeptide). The two main secondary structures are  $\alpha$ -helix and  $\beta$ -sheet, which are observed in polypeptide solutions [1, 21] and polypeptide multilayers [1–3, 9, 22–24]. The tertiary structure of the polypeptide reflects how secondary structures organize relative to each other to form overall globular, fibrous, or random polypeptide structure. Quaternary structure occurs when whole polypeptides interact with each other to provide a unique structure or biological activity.

**Table 1.** Structural formulas of the 20 usual amino acids.

Amino acids with hydrophilic side groups:				
$\begin{array}{c} \text{COO}^- \\   \\ ^+\text{H}_3\text{N}-\text{C}-\text{H} \\   \\ \text{CH}_2 \\   \\ \text{C} \\ / \quad \backslash \\ \text{H}_2\text{N} \quad \text{O} \end{array}$ <p><b>Asparagine (N)</b></p>	$\begin{array}{c} \text{COO}^- \\   \\ ^+\text{H}_3\text{N}-\text{C}-\text{H} \\   \\ \text{CH}_2 \\   \\ \text{CH}_2 \\   \\ \text{COO}^- \end{array}$ <p><b>Glutamic acid (E)</b></p>	$\begin{array}{c} \text{COO}^- \\   \\ ^+\text{H}_3\text{N}-\text{C}-\text{H} \\   \\ \text{CH}_2 \\   \\ \text{CH}_2 \\   \\ \text{C} \\ / \quad \backslash \\ \text{H}_2\text{N} \quad \text{O} \end{array}$ <p><b>Glutamine (Q)</b></p>	$\begin{array}{c} \text{COO}^- \\   \\ ^+\text{H}_3\text{N}-\text{C}-\text{H} \\   \\ \text{CH}_2 \\   \\ \text{C}=\text{N}^+ \\    \quad \backslash \\ \text{HC} \quad \text{CH} \\   \\ \text{H} \end{array}$ <p><b>Histidine (H)</b></p>	$\begin{array}{c} \text{COO}^- \\   \\ ^+\text{H}_3\text{N}-\text{C}-\text{H} \\   \\ \text{CH}_2 \\   \\ \text{CH}_2 \\   \\ \text{CH}_2 \\   \\ \text{CH}_2 \\   \\ \text{NH}_3^+ \end{array}$ <p><b>Lysine (K)</b></p>
$\begin{array}{c} \text{COO}^- \\   \\ ^+\text{H}_3\text{N}-\text{C}-\text{H} \\   \\ \text{CH}_2 \\   \\ \text{CH}_2 \\   \\ \text{CH}_2 \\   \\ \text{NH} \\   \\ \text{C}=\text{NH}_2^+ \\   \\ \text{NH}_2 \end{array}$ <p><b>Arginine (R)</b></p>	$\begin{array}{c} \text{COO}^- \\   \\ ^+\text{H}_3\text{N}-\text{C}-\text{H} \\   \\ \text{CH}_2 \\   \\ \text{COO}^- \end{array}$ <p><b>Aspartic acid (D)</b></p>			
Amino acids with hydrophobic side groups:				
$\begin{array}{c} \text{COO}^- \\   \\ ^+\text{H}_3\text{N}-\text{C}-\text{H} \\   \\ \text{CH} \\ / \quad \backslash \\ \text{H}_3\text{C} \quad \text{CH}_3 \end{array}$ <p><b>Valine (V)</b></p>	$\begin{array}{c} \text{COO}^- \\   \\ ^+\text{H}_3\text{N}-\text{C}-\text{H} \\   \\ \text{CH}_2 \\   \\ \text{CH} \\ / \quad \backslash \\ \text{H}_3\text{C} \quad \text{CH}_3 \end{array}$ <p><b>Leucine (L)</b></p>	$\begin{array}{c} \text{COO}^- \\   \\ ^+\text{H}_3\text{N}-\text{C}-\text{H} \\   \\ \text{H}-\text{C}-\text{CH}_3 \\   \\ \text{CH}_2 \\   \\ \text{CH}_3 \end{array}$ <p><b>Isoleucine (I)</b></p>	$\begin{array}{c} \text{COO}^- \\   \\ ^+\text{H}_3\text{N}-\text{C}-\text{H} \\   \\ \text{CH}_2 \\   \\ \text{CH}_2 \\   \\ \text{S} \\   \\ \text{CH}_3 \end{array}$ <p><b>Methionine (M)</b></p>	$\begin{array}{c} \text{COO}^- \\   \\ ^+\text{H}_3\text{N}-\text{C}-\text{H} \\   \\ \text{CH}_2 \\   \\ \text{C}_6\text{H}_5 \end{array}$ <p><b>Phenylalanine (F)</b></p>
Amino acids that are in between:				
$\begin{array}{c} \text{COO}^- \\   \\ ^+\text{H}_3\text{N}-\text{C}-\text{H} \\   \\ \text{H} \end{array}$ <p><b>Glycine (G)</b></p>	$\begin{array}{c} \text{COO}^- \\   \\ ^+\text{H}_3\text{N}-\text{C}-\text{H} \\   \\ \text{CH}_3 \end{array}$ <p><b>Alanine (A)</b></p>	$\begin{array}{c} \text{COO}^- \\   \\ ^+\text{H}_3\text{N}-\text{C}-\text{H} \\   \\ \text{H}-\text{C}-\text{OH} \\   \\ \text{H} \end{array}$ <p><b>Serine (S)</b></p>	$\begin{array}{c} \text{COO}^- \\   \\ ^+\text{H}_3\text{N}-\text{C}-\text{H} \\   \\ \text{H}-\text{C}-\text{OH} \\   \\ \text{CH}_3 \end{array}$ <p><b>Threonine (T)</b></p>	$\begin{array}{c} \text{COO}^- \\   \\ ^+\text{H}_3\text{N}-\text{C}-\text{H} \\   \\ \text{CH}_2 \\   \\ \text{C}_6\text{H}_4 \\   \\ \text{OH} \end{array}$ <p><b>Tyrosine (Y)</b></p>
$\begin{array}{c} \text{COO}^- \\   \\ ^+\text{H}_3\text{N}-\text{C}-\text{H} \\   \\ \text{CH}_2 \\   \\ \text{C} \\ / \quad \backslash \\ \text{HC} \quad \text{N} \\   \quad \backslash \\ \text{H} \quad \text{C}_6\text{H}_5 \end{array}$ <p><b>Tryptophan (W)</b></p>	$\begin{array}{c} \text{COO}^- \\   \\ ^+\text{H}_3\text{N}-\text{C}-\text{H} \\   \\ \text{CH}_2 \\   \\ \text{SH} \end{array}$ <p><b>Cysteine (C)</b></p>	$\begin{array}{c} \text{COO}^- \\   \\ ^+\text{H}_2\text{N}-\text{C}-\text{H} \\   \\ \text{H}_2\text{C} \\   \\ \text{C} \\   \\ \text{H}_2 \end{array}$ <p><b>Proline (P)</b></p>		

Polypeptides constitute ~50% of the dry mass of a living organism [25] and are, therefore, particularly well suited for the development of biocompatible films and coatings. Polypeptides have been used as a raw material for products in pharmaceuticals, food science, and waste disposal [26].

Polypeptides are distinguished from non-polypeptide polyelectrolytes in various ways. For instance, some monomers are particularly reactive (e.g., the thiol group of cysteine, important in some mechanisms of enzyme catalysis). It is possible to prepare monodisperse samples under favorable conditions, the polymer sequence can be designed as desired, and the stiffness of the polymer backbone is intrinsically high due to the rigidity of the peptide bonds.



**Scheme 1.** Formation of a tetrapeptide from four amino acids.

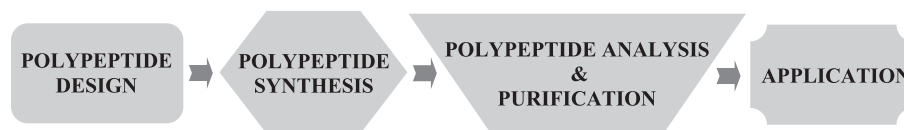
## 2.2. Chemical Synthesis of Polypeptides

Two chemical synthesis methods, i.e., solid phase and solution phase peptide synthesis, are widely used to acquire polypeptides. Scheme 2 diagrams the steps involved in obtaining a synthetic polypeptide.

### 2.2.1. Solid Phase Peptide Synthesis

In 1963, American chemist Bruce Merrifield at Rockefeller University introduced solid phase peptide synthesis. Merrifield was awarded the Nobel Prize in 1984 for his contribution to the advancement of peptide chemistry.

Solid phase peptide synthesis uses a polymer with reactive sites (solid supports, insoluble resin supports) that chemically combines with the developing polypeptide chain. It consists of two distinct sets of operations: (1) chain assembly on a resin and (2) simultaneous or sequential cleavage and deprotection of the resin-bound, fully protected chain. Various chemical strategies exist for the chain assembly and cleavage/deprotection operations. The two major chemistries for solid phase peptide synthesis are Fmoc and t-Boc. Each method involves fundamentally different amino acid side-chain protection, consequent cleavage/deprotection methods, and resins; the t-Boc method requires the use of stronger HF containing anisole alone or anisole plus other scavengers, whereas polypeptide resins produced by Fmoc chemistry are usually cleaved by less harsh reagents K or R. Fmoc chemistry is known for polypeptide synthesis of higher quality and in greater yield than t-Boc chemistry. After synthesis, polypeptides are usually purified by reversed-phase high performance liquid chromatography and characterized by mass spectrometry.



**Scheme 2.** Diagram of the steps involved in obtaining a synthetic polypeptide.

### 2.2.2. Solution Phase Peptide Synthesis

Solution phase peptide synthesis is not used as widely as the solid phase method. Solution phase peptide synthesis may be applicable for polypeptides that are longer than 100 amino acids or for large-scale synthesis of well-known polypeptides. PLL and PLGA, commercially available with different molecular weights, are usually made from solution phase peptide synthesis and the products are polydisperse. Solution phase peptide synthesis is usually labor-, time-, and skill-intensive largely due to the unpredictable solubility characteristics of intermediates.

Different from the aforementioned chemical synthesis methods, recombinant synthesis (or microbial or biotic synthesis) is based on gene synthesis technology. It has been used in recent years for the production of proteins or polypeptides with high molecular weights.

## 3. TECHNIQUES FOR FABRICATION OF POLYPEPTIDE MULTILAYERS

Chemists have used a variety of techniques, e.g., thermal evaporation, sputtering, electrodeposition, molecular beam epitaxy, adsorption from solution, LB technique, and LBL, to fabricate multilayer films and coatings on solid substrates. Among these, the LB and LBL techniques are the two most well known for preparing polypeptide multilayers.

### 3.1. Langmuir-Blodgett (LB) Technique

The term LB comes from the names of a research scientist and his assistant, Irving Langmuir and Katherine Blodgett, who discovered unique properties of thin films in the early 1900s. Langmuir's original work involved the transfer of monolayers from liquid to solid substrates. He was awarded the Nobel Prize for his systematic studies on monolayers. Several years later, Blodgett expanded on Langmuir's research to deposit multilayer films on solid substrates [27]. After the pioneering work done by Langmuir and Blodgett, it took almost half a century before scientists worldwide started to realize the potential of this unique technique.

Scheme 3 displays the LB deposition process [28]. One molecular layer is formed by dipping a solid substrate into water containing a polymer, i.e., subphase, that forms a single layer of molecular chains on the surface [Scheme 3a]. This layer is then transferred from the water to the substrate. An ordered, multilayer film can be created by repeating the dipping process [Scheme 3b]. There are a variety of dipping schemes resulting in predominantly three types of LB multilayer films. The most common is the Y-type multilayer, which is produced when the monolayer deposits to the solid substrate in both up and down directions. When the monolayer deposits only in one direction (down or up), the multilayer structure is called either X-type or Z-type [Scheme 3b].

Many factors may influence the film-forming characteristics:

- subphase composition and temperature,
- pH of subphase,
- purity of subphase,
- addition of ions to stabilize films,
- nature of the spread film, and
- type and nature of the solid substrate.

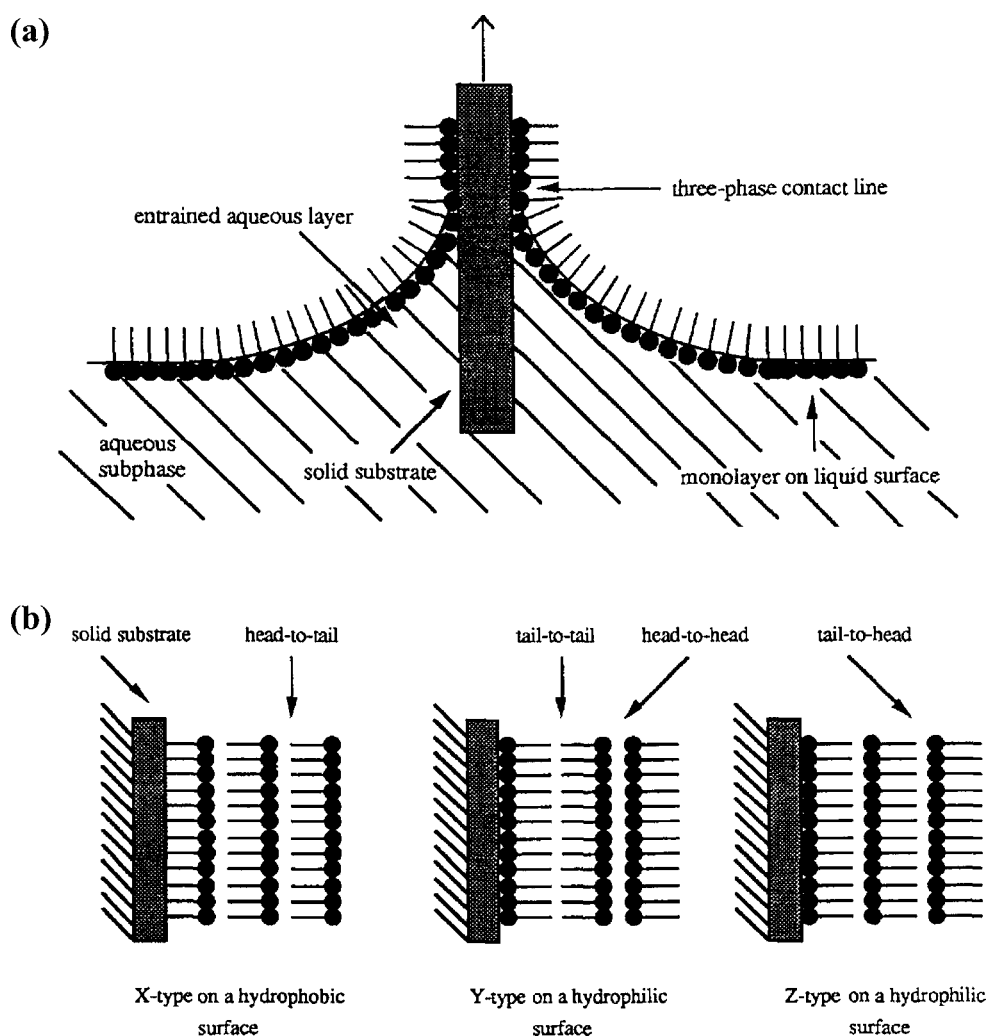
The main advantages of LB over other methods are its ability to offer an enhanced degree of order and packing density and its ability to form oriented monolayers of molecules whose activity may exceed that of those immobilized by other methods. However, this technique has difficulties in assemblies on substrates with irregular shape, and it needs a complicated setup to form alternating multilayers.

### 3.2. Electrostatic Layer-by-Layer (LBL) Self-Assembly

LBL is the most promising method for preparation of multilayer nanofilms of controlled thickness and molecular architecture. This method was pioneered by Iler [14] and extended as a new ultrathin film preparation by Decher et al. in the early 1990s [15].

LBL has been used to make polyelectrolyte multilayer films, coatings, and microcapsules from oppositely charged polymers [1, 2, 15, 16, 29–43]. The procedure involves the repetitive sequential dipping of a substrate in solutions of oppositely charged polyelectrolytes. On adsorption, the





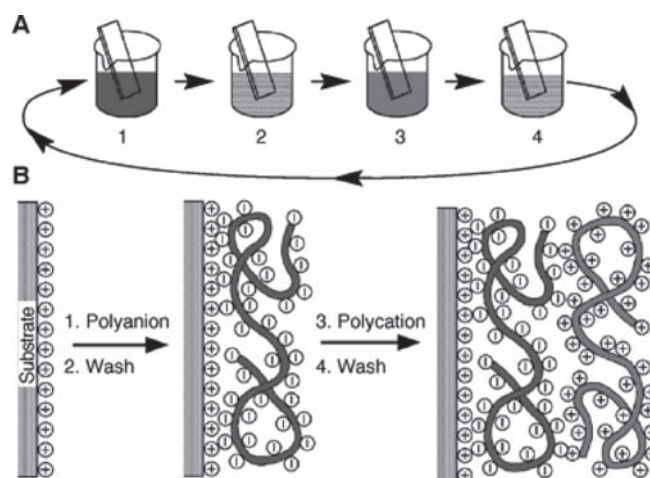
**Scheme 3.** (a) Deposition of a floating monolayer on a solid substrate, and (b) different types of LB deposition. Alternating multilayers can also be built up. Reprinted with permission from [28], B. P. Binks, *Adv. Colloid Interface Sci.* 34, 343 (1991). © 1991, Elsevier.

polymers become kinetically trapped; the surface charge is reversed after each cycle. Each layer can have a thickness on the order of nanometers, typically 1–2 nm, enabling the design and engineering of surfaces and interfaces at the molecular level. As shown in Scheme 4, the LBL multilayer fabrication process can be generally described as follows: (i) prepare solutions of polycation and polyanion, (ii) alternately immerse the substrate in these solutions for 20 min, (iii) rinse the substrate for several seconds after each deposition step, and (iv) monitor the deposition of materials on the substrate using various techniques that will be described.

A variety of materials have been used for LBL multilayers. These materials include functional polymers [44, 45], biopolymers [46–48], inorganic materials [49, 50], and small molecules [51, 52]. Recently, polypeptide and protein multilayers have attracted remarkable interest [1, 2, 8, 9, 30, 36, 53–57].

The physical basis of LBL is mainly electrostatic attraction [15]. However, other forces, e.g., hydrophobic, van der Waals, and hydrogen bonding or acid-base type, may also play a significant role in certain systems. For instance, multilayers have been formed based on hydrogen bonding [58–62], and, in the case of biomolecules, multilayers of streptavidin and biotinylated PLL [63] and multilayers of Con A and glycogen (branched polyglucose) [64] have been prepared based on bio-specific interactions.

The properties of LBL multilayers can easily be manipulated. Variables include choice of substrate, solution conditions (i.e., concentration, pH, ionic strength, temperature), polyelectrolyte structure, and method of post-fabrication functionalization. For instance, the solution pH of weak



**Scheme 4.** (A) Schematic of the LBL film deposition process using slides and beakers. Steps 1 and 3 represent the adsorption of a polyanion and polycation, respectively, and steps 2 and 4 are washing steps. The four steps are the basic buildup sequence for the simplest film architecture,  $(A/B)_n$ . The construction of more complex film architectures requires only additional beakers and a different deposition sequence. (B) Simplified molecular picture of the first two adsorption steps depicting film deposition starting with a positively charged substrate. Counterions are omitted for clarity. The polyon conformation and layer interpenetration are an idealization of the surface charge reversal with each adsorption step. Reprinted with permission from [15], G. Decher, *Science* 277, 1232 (1997). © 1997, AAAS.

polyelectrolytes strongly influences the multilayer surface friction, roughness, morphology, and dielectric properties [65–70]. The solution pH of weak polyelectrolytes may also influence the film thickness [66, 71–74], polymer interpenetration and surface wettability [65], film stability [34, 36, 67, 75–77], and permeability [78, 79].

LBL holds much promise for commercial use of multilayer films and microcapsules in the fields of medicine, optics, light-emitting devices, sensors, and nanoreactors [80–84]. Compared to other methods of multilayer formation, LBL has great advantages: it provides a rather simple aqueous-based means while providing enormous design flexibility, including the ability to create complex multilayer heterostructures [43]. Moreover, films prepared by LBL can feature nanometer-scale organization, controlled thickness and film composition, and designed supramolecular architecture. The repetitiveness of the layering process is suitable for automation, which is important for commercialization prospects. Finally, LBL can be used to deposit multilayers on almost any kind of solid substrate.

#### 4. TECHNIQUES FOR MONITORING AND CHARACTERIZING POLYPEPTIDE MULTILAYER FORMATION

A number of techniques have been used to study the formation of polypeptide and non-polypeptide multilayers. These include quartz crystal microbalance (QCM), UV-vis, atomic force microscopy (AFM), fluorescence microscopy, ellipsometry, Fourier transform infrared spectroscopy (FTIR), and circular dichroism (CD) spectroscopy.

##### 4.1. Quartz Crystal Microbalance (QCM)

QCM is a sensitive tool for analyzing polypeptide multilayers [1, 30, 54, 85]; it is an easy in situ technique to detect the adsorption of polypeptides during the self-assembly process. QCM is based on the property of quartz oscillators to change their frequency linearly proportional to the deposited mass according to the Sauerbrey equation [86]. Adsorption of polypeptides can be observed quantitatively at the nanogram level [1, 16, 30, 54, 85, 87–89].

##### 4.2. UV-Vis

UV-vis spectroscopy is one of the truly routine techniques in modern biochemistry, biology, and pharmaceutical research. UV-vis spectroscopy is the measurement of the wavelength and



intensity of absorption of near-ultraviolet and visible light by a sample. An absorption spectrum shows a number of absorption bands corresponding to structural groups within the molecule. Any species with an extended system of alternating double and single bonds absorb UV light, and anything with color absorbs visible light, making UV-vis spectroscopy applicable to a wide range of samples. Because of its wide availability, UV-vis has been widely used for monitoring the formation of polypeptide multilayers [2, 16, 51]. Note that UV-vis spectra have broad features that are of limited use for sample identification but are very useful for quantitative measurements as the absorbance of a sample increases with its concentration.

#### 4.3. Atomic Force Microscopy (AFM)

AFM is one of the most versatile types of scanning probe microscopes. It is an imaging technique that, in some cases, can resolve atomic lattice in the real space. To use this system, a cantilever tip is brought in contact with the surface of a solid sample. As the tip nears the sample surface, some repulsive force between the tip and the surface appears. This force from the surface applied on the cantilever tip bends the cantilever upward. A laser beam is reflected over the cantilever, forming a spot that is reflected on a split photodetector. The photodetector monitors the bending of the cantilever and can be used to calculate the force. Keeping the force constant while scanning the tip across the surface, the vertical movement of the tip follows the surface profile, which is then recorded as the surface topography. AFM has been used to investigate the surface morphology of polypeptide multilayers [2, 16, 36] and protein film structure [90–92].

#### 4.4. Fluorescence Microscopy

Fluorescence is the property of some atoms and molecules to absorb light at a particular wavelength and to subsequently emit light of longer wavelength after a brief interval. A certain type of dye attaches a polypeptide molecule; fluorescence reveals the adsorption of this polypeptide molecule. Using this technique, fluorescent-labeled polypeptide microcapsules have been visualized [93].

#### 4.5. Ellipsometry

Ellipsometry is also a sensitive optical method for measuring properties such as the thickness and refractive index of thin films at interfaces. This method has been used for nearly one hundred years to derive information about surfaces. It makes use of the fact that the polarization state of light may change when the light beam is reflected from a surface. If the surface is covered by a polypeptide thin multilayer, the entire optical system of multilayers and substrates influences the change in polarization. It is therefore possible to deduce information about the polypeptide multilayer properties including thickness. Using ellipsometry, the thickness and refractive index of multilayers made of designed polypeptides [16] and the buildup and stability of PLL/PLGA multilayers [56, 85] have been studied.

#### 4.6. Fourier Transform Infrared Spectroscopy (FTIR)

FTIR is perhaps the most powerful tool for identifying types of chemical bonds (functional groups). This technique measures the absorption of various infrared light wavelengths by the material of interest. Because chemical bonds absorb infrared energy at specific wavelengths, the basic structure of compounds can be determined by the spectral locations of their infrared absorptions. For most common materials, the spectrum of an unknown can be identified by comparison to a library of known compounds. FTIR has been used to study the secondary structure of PLL/PLGA multilayers [9, 12, 55, 94]. FTIR can also be used for some quantitative analyses because the strength of the absorption is proportional to concentration. FTIR has been used to monitor the assembly process of polypeptide multilayers [1]; the absorption intensity of a certain characteristic peak, such as Amide I, increases with adsorption steps.

#### 4.7. Circular Dichroism (CD) Spectroscopy

CD spectroscopy is another technique that has been used to characterize the secondary structure of polypeptides [1, 21, 95, 96] and polypeptide multilayers [1, 30, 36, 51]. CD measures the differences in the absorption of left-handed polarized light versus right-handed polarized light that arise due to structural asymmetry. The absence of regular structure results in zero CD intensity, while an ordered structure results in a spectrum that can contain both positive and negative

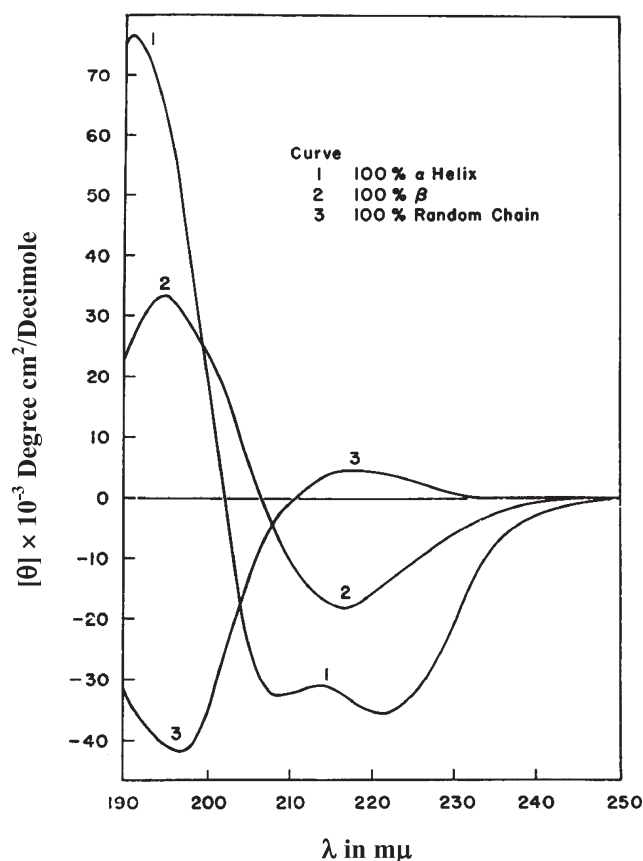


**Figure 1.** Circular dichroism spectra of PLL in the  $\alpha$ -helix,  $\beta$ -sheet, and random coil conformation. Reprinted with permission from [97], N. J. Greenfield and G. D. Fasman, *Biochemistry* 8, 4108 (1969). © 1969, American Chemical Society.

signals. The secondary structure of polypeptide multilayers can be determined by CD in the far-UV spectral region (190–250 nm). At these wavelengths, the chromophore is the peptide bond.  $\alpha$ -helix,  $\beta$ -sheet, and random coil structures each give rise to a characteristic shape and magnitude on the CD spectrum. Figure 1 shows the spectra for PLL in these three different conformations [97]. The approximate fraction of each secondary structure type that is present in any polypeptide or protein can thus be determined by analyzing its far-UV CD spectrum as a sum of fractional multiples of such reference spectra for each structural type. A predominant  $\beta$ -sheet structure has been observed in multilayer films of designed polypeptides [1, 30, 98]. Note that CD and FTIR are the two main techniques that have been useful for the study of the secondary structure of polypeptide multilayers. In the analysis of film structure by FTIR, the Amide I band is decomposed into contributions corresponding to the various types of secondary structure. Due to extensive band overlapping in the FTIR spectrum, however, it can be difficult and inaccurate to assign a unique absorption band to a certain structural group; CD could be more accurate in the determination of secondary structure, while FTIR remains a precious tool for the identification of chemical bonds.

Other techniques, e.g., cyclic voltammetry [53, 54], surface profilometry [16], and X-ray diffraction [23], can also be used to monitor the formation of polypeptide multilayers. These techniques are complementary; they can provide different information about the polypeptide multilayers.

## 5. POLYPEPTIDE MULTILAYER FILMS AND MICROCAPSULES

As described above, polypeptide multilayers have been mainly prepared by two methods: LB [22, 23, 57] and LBL [1, 8, 9, 30, 53, 54, 89]. The latter, since its introduction in 1991, has provided novel opportunities for fabricating functional multilayer films and microcapsules. LBL has been extensively studied for multilayer films and microcapsules from non-polypeptide polyelectrolytes

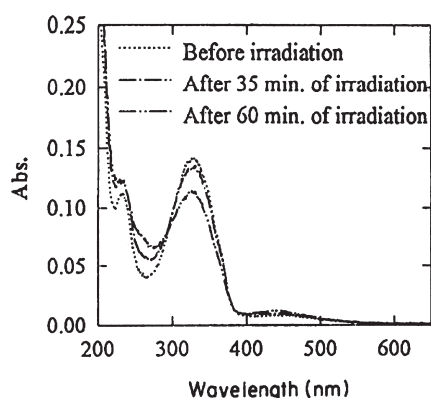


**Figure 2.** Photo-responsive behavior of LB multilayer films after irradiation times of 35 and 60 min. Reprinted with permission from [57], C. Tedeschi et al., *Thin Solid Films* 284–285, 174 (1996). © 1996, Elsevier.

[82, 99]. It has been getting more and more attention in a variety of biological macromolecules such as polypeptides [1, 9, 30] and nucleic acids [100–102]. What has been learned about multilayers from non-polypeptide polyelectrolytes, including weak ones, may not be suitable to predict properties, including biological properties, of polypeptide multilayers.

### 5.1. Polypeptide Multilayer Films Prepared Using LB Technique

Most polypeptides can be adjusted to be anionically or cationically charged by simply adjusting the solution pH to be higher or lower than the isoelectric point. This property has been previously applied in LB technique to build a composite lipid/enzyme monolayer structure at the air-water interface [103]. The monolayers can be transferred onto a solid planar substrate to build multilayer assemblies.

Poly( $\gamma$ -methyl-L-glutamate) multilayers have been prepared using the LB technique, and  $\alpha$ -helical structure has been observed [22]. Highly ordered polypeptide multilayer films have also been fabricated from chloroform solutions of PLGA derivatives [23], which are deposited onto solid substrates (e.g., glass slides) by the vertical dipping method as Z-type films with almost unity ratio. FTIR, X-ray diffraction, and CD measurements show that these polypeptide multilayers have  $\alpha$ -helix structure. Functional organic molecules such as phthalocyaninato metals have been deposited onto the ordered LB multilayer films, and the in-plane electrical conductivity of the multilayer thin films can be as high as  $10^{-4}$  S cm $^{-1}$  after doping with I $_2$ .

Polypeptide multilayers with controlled aggregation of photochromic compounds have also been developed [57]. Azopoly-L-lysine, which has photochromic behavior associated with the trans  $\rightleftharpoons$  cis photoisomerization of the azobenzene units, has been used. Up to seven layers of azopoly-L-lysine have been deposited, and the optical absorption studies have shown linearity between optical density and number of layers. The phototropism of the azopoly-L-lysine is preserved in the solid LB multilayer films [Figure 2]. Such polypeptide multilayers are potentially useful for optoelectronic applications such as optical data storage [104].

### 5.2. LBL Multilayers of Poly(L-lysine)/Poly(L-glutamic acid)

PLL and PLGA are polydisperse; one advantage of using PLL and PLGA is their commercial availability. Because of their biocompatibility and biodegradability, PLL/PLGA multilayers are of great interest for medical applications such as coatings for biomaterials in implant technology.

#### 5.2.1. Assembly Behavior

Polypeptide multilayers of PLL and PLGA have been developed using the LBL technique [8, 9, 53, 54, 89]. Two types of assembly behavior are observed during LBL polyelectrolyte multilayers: those whose mass and film thickness increase linearly with the number of layers [1, 30, 105–107] and those whose mass and film thickness increase superlinearly or exponentially [9, 53–55, 85, 88, 108, 109].

The first film type (linear increase) has been mainly observed when the two polyelectrolytes, polypeptides or non-polypeptides, are fully charged such as two strong polyelectrolytes or two fully charged weak polyelectrolytes. Under such conditions, the thickness per bilayer is small; the resulting film is dense and presents a periodic structure where the interactions of each layer

are constrained to its neighbors [15]. Therefore, the polyelectrolytes from the solution interact only with the outer part of the multilayer and do not interact with polyelectrolyte layers more deeply embedded in the film, and, therefore, the film grows linearly [1, 30, 105–107].

Multilayers made of at least one weak polyelectrolyte may grow superlinearly or exponentially. Hoffmannová et al. have observed that the mass of PLL/PLGA deposited increases superlinearly with increasing adsorption cycles, and much more PLL than PLGA is deposited in each cycle [54]. These findings are consistent with the observation by Cheng and Corn, who have found that PLL layers are thicker on average than PLGA layers [53]. Similar mass increment behavior has been observed by Halthur and Elofsson [85]. This exponential growth is believed to be due to the diffusion in and out through the whole film at each adsorption cycle of at least one of the two polyelectrolyte components [109].

The film density of PLL/PLGA multilayers has been studied during the assembly process [85]. The measurements of the refractive index and the water content in the multilayers have shown that the density of PLL/PLGA multilayers increases with increasing adsorption cycles. This increase in film density is proposed as a result of polymers diffusing into and attaching inside the underlying layers.

The mass deposition of polypeptides may depend on the properties of the buffer present in the polypeptide solutions [54]. At pH 8.5, the PLL/PLGA multilayers grown in phosphate buffers show a mass twice that of the corresponding films grown in carbonate buffer. However, it should be noted that in these experiments [54], the concentration for the two buffers are very different (0.005 M for carbonate buffer and 0.02 or 0.1 M for phosphate buffer). This changes the ionic strength, and, therefore, could have a big influence on the assembly behavior.

The influence of pH on the buildup of PLL/PLGA multilayers has been studied from pH 1.5 to 11.3 by Boulmedais et al. [Figure 3] [55]. The multilayer film thickness is the largest when the multilayers are built under acidic (e.g., pH 1.5) or alkaline (e.g., pH 10.4) conditions (except for pH exceeding 10.4). The smallest film thickness is at pH 4.4 and 7.4. Similar results have been observed in poly(allylamine hydrochloride)/poly(acrylic acid) multilayers prepared in the absence of salt [110]. This effect is explained by the fact that when one of the polyelectrolytes is not fully charged, for instance, PLGA at acidic and PLL at alkaline conditions, it interacts with the outer oppositely charged surface by forming loops that extend into the solution. This leads to larger film thickness and also, usually, to more material being deposited. At the intermediate pH values, i.e., pH 4.4 and 7.4, most residues on both PLL and PLGA are charged, the interactions between PLL and PLGA are strong, and, therefore, induce a small thickness increase per bilayer.

The influence of pH on PLL/PLGA multilayer formation has also been studied by Haynie et al. [89]. They have found that pH controls the assembly behavior of PLL/PLGA multilayers in the range of pH 4–10.5, and pH can be used to control the secondary structure content of PLL/PLGA multilayers following fabrication at neutral pH [36, 89].

Cheng and Corn have also observed the difference in thickness of PLL/PLGA multilayers made from pH 5.6 to 9.4 [53]. The thickness of the eight-layer PLL/PLGA multilayer at pH 9.4 is 24%

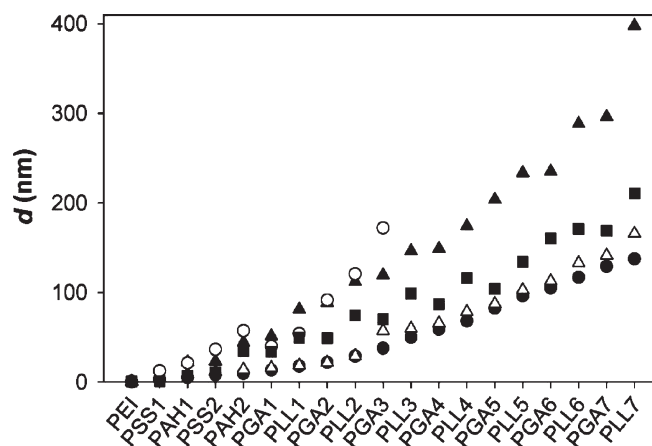


**Figure 3.** Evolution of the multilayer thickness  $d$  during the buildup process of a PEI-(PSS-PAH)<sub>2</sub>-(PLGA-PLL)<sub>7</sub> multilayer followed by optical waveguide light mode spectroscopy at different pHs: (○) pH 1.5, (●) pH 4.4, (△) pH 7.4, (▲) pH 10.4, and (■) pH 11.3. Data for pH 8.4 are not represented due to poor experimental reproducibility. Reprinted with permission from [55], F. Boulmedais et al., *Langmuir* 19, 9873 (2003). © 2003, American Chemical Society.

greater than the multilayer fabricated from pH 8.0, and the eight-layer film created at pH 5.4 is 10% thinner than at pH 8.0. Also, for all pH solutions used, the thickness of a PLL layer is greater than that of a PLGA layer. Because the operating pH values (5.6, 8.0, and 9.4) are within the  $pK_a$ s range of PLGA (4.9) and PLL (10.5), the vast majority of the residues on both PLL and PLGA are charged. It seems that the variations in the film thickness with solution pH in this range should not be so large. Therefore, it is believed that the change in film thickness at these pH ranges is not simply related to the solution pH; it may also be related to the intrinsic structure, e.g., hydrophobicity, of the PLL polycation relative to the PLGA polyanion.

Note that most PLL/PLGA multilayers have been fabricated with pre-layers of non-polypeptide polyelectrolytes [8, 9, 55, 85]. The assembly behavior with and without pre-layers has been discussed by Halthur and Elofsson [85]; they have shown that the buildup of polypeptide multilayers is sensitive to the pre-layers. The use of pre-layers of non-polypeptide polyelectrolytes such as polyethylimine (PEI) induces a difference in the thickness increments for PLL (40–55 Å/layer) and PLGA (25–35 Å/layer) in the first several layers, whereas this difference diminishes when the influence of PEI pre-layers is omitted.

### 5.2.2. Film Stability

The stability of polypeptide multilayers is important not only in terms of construction and storage, but also for understanding how the polypeptide multilayer reacts when in contact with various environments. The stability of polypeptide multilayers could depend on pH, temperature, or solvent. At neutral pH, the vast majority of the residues on both PLL and PLGA are charged, and the cooperative electrostatic interaction between PLL and PLGA is strong and can prevent dissociation of PLL/PLGA multilayers. However, under certain physical or chemical conditions, a polypeptide multilayer could show an undesirable tendency to disintegrate [36].

The stability of PLL/PLGA multilayers has been investigated by means of in situ ellipsometry [56]. The effects of drying/rewetting and changes in temperature and pH after the LBL process have been studied by continuously monitoring the thickness, refractive index, and adsorbed mass of the multilayers. It was found that the thickness of a PLL/PLGA multilayer assembled decreases remarkably, approximately 70%, upon drying [Figure 4], and the thickness in the dry state is extremely sensitive to ambient humidity. Upon rewetting of the dry sample, the original thickness can be re-established [56].

Changes in temperature (25–37°C) may induce changes in thickness by as much as 8% [56]. Multilayers formed at higher temperatures yield thicker films due to changes in polymer-solution interactions [111] and probably even more so due to polyelectrolytes having a higher internal mobility at higher temperatures, which enables them to swell into conformations that are unfavorable at lower temperatures [112]. The temperature-induced changes in secondary structure can also contribute to a change in polypeptide multilayer thickness.

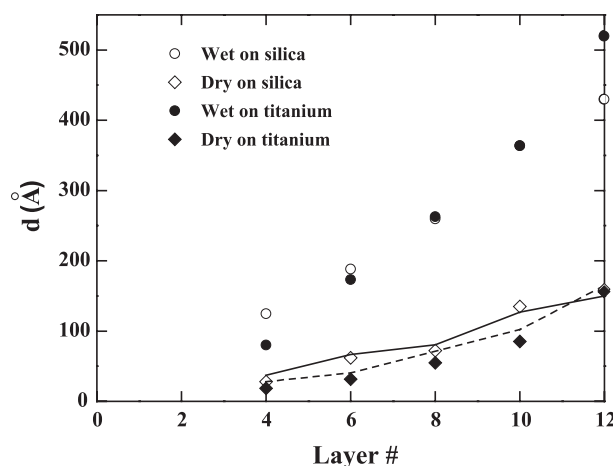


**Figure 4.** Polyelectrolyte multilayer film in the wet (circles) and dry (diamonds) state. Thickness of films, built on silica and titanium surfaces (unfilled and filled symbols, respectively). The lines are the thickness calculated with a constant refractive index (1.52). Reprinted with permission from [56], T. J. Halthur et al., *J. Am. Chem. Soc.* 126, 17009 (2004). © 2004, American Chemical Society.

A more obvious change in thickness has been observed by changing the solution pH. The change in pH (3.9–10.1) enables the PLL/PLGA multilayers to undergo a nonreversible swelling/deswelling behavior, and a change of up to 10–20% has been reported [56]. A similar phenomenon has been observed in PLL/hyaluronic acid multilayers, where the multilayers swell one to eight times when they are immersed in solutions of different pH [70].

Several research groups [36, 55] have reported the dissociation of PLL/PLGA multilayers related to pH jumps. Boulmedais et al. have observed that PLL/PLGA multilayers undergo a partial dissociation on contact with a solution of pH 1.5, and complete dissolution has been observed upon immersion into a solution of pH 13.0 [55]. Zhi and Haynie have reported that PLL/PLGA multilayers dissociate about 8% at pH 2.0 and more than 30% at pH 12.0 [36]. The influence of pH on polypeptide multilayer stability is probably governed by two main factors: the loss and gain of charge density and changes in secondary structure. Both might lead to structural changes in the polypeptide multilayer. At an extreme pH, i.e., strong acid or base, either PLGA or PLL becomes uncharged or less charged, and the other component molecules become fully charged and repel themselves. This repulsion leads to multilayer dissociation.

### 5.2.3. Secondary Structure and Structural Stability

Polypeptides are known to interact not only through electrostatic interactions but also through hydrogen bonding. Their chemical nature allows them to form secondary structures such as  $\alpha$ -helices and  $\beta$ -sheets. At the same time, polyelectrolyte multilayers are known to preserve the secondary structure of proteins [10], and the helical structure of DNA [101] or PLL [113, 114]. Cooper et al. have reported that the interactions between PLL and Congo Red dye lead to  $\alpha$ -helical structures [51], and the interactions of PLL and PLGA result in a mixture of  $\alpha$ -helices and  $\beta$ -sheets [24]. Boulmedais et al. have shown that it is possible to develop polypeptide multilayers with significant secondary structure content such as  $\alpha$ -helices and  $\beta$ -sheets [9]. They have also shown that the precursor layers, i.e., two bilayers of poly(allylamine hydrochloride)/poly(styrene sulfonate) PAH/PSS, only influence the secondary structure of PLL/PLGA multilayers in the first few bilayers. The  $\beta$ -sheet content increases at the expense of random coil with an increasing number of bilayers; except this is not the case for pH 1.5, where no  $\beta$ -sheet contribution has been observed. After several bilayers, the secondary structures of the PLL/PLGA multilayers become independent of the number of bilayers [55]. All of these have shown that local order can be generated in polypeptide multilayers by specific interactions between polycations and polyanions.

Boulmedais et al. have also compared the secondary structures of polypeptide multilayers with the corresponding complexes in solution using FTIR [9, 55]. Two kinds of experiments have been carried out. In one set of experiments [9], they have compared the secondary structures of PLL/PLGA complexes in solution at various pH values to those of the corresponding PLL/PLGA multilayers [Figure 5]. In the other set of experiments [55], the secondary structures of complexes

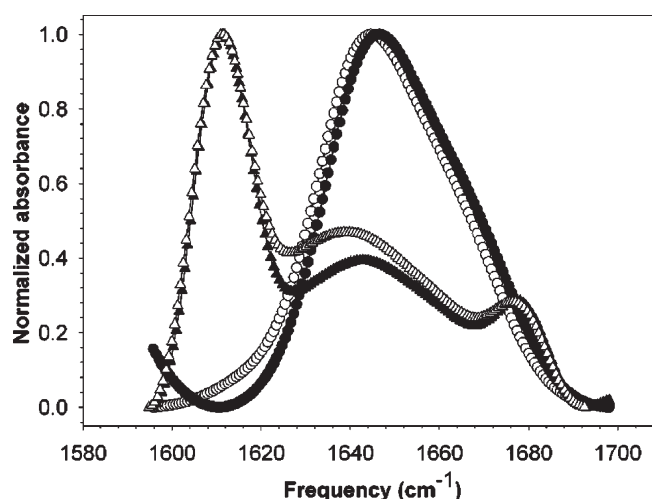


**Figure 5.** Normalized infrared absorption spectra of PLL (○), PLGA (●), PLGA-PLL complexes (▲) in solution and a (PLGA-PLL)<sub>7</sub> multilayer (△) deposited on its precursor film, measured at pH 8.4 in deuterated Mes-Tris buffer. Reprinted with permission from [9], F. Boulmedais et al., *Langmuir* 18, 4523 (2002). © 2002, American Chemical Society.



and multilayers have been studied for various polyanion/polycation systems at a given pH. For instance, poly(L-aspartic acid)/PLL and PLGA/poly(L-ornithine) systems have been studied at pH 7.4; poly(L-aspartic acid) and poly(L-ornithine) differ from PLGA and PLL, respectively, by the reduction of the side chains by one methylene group. Moreover, PLL has been replaced with poly(D-lysine), which has different chirality. In all the systems studied, the secondary structures of polypeptide multilayers always closely resemble those of the corresponding complexes in solution [55, 115].

The stability in the local order structure of PLL/PLGA multilayers toward external stresses such as pH jumps and temperature rise has been studied [36, 55]. It has been found that the secondary structures of PLL/PLGA multilayers appear very stable against pH jumps in the range of pH 4–10.5;  $\beta$ -sheets stabilize the polypeptide multilayers. However, the sudden exposure of a PLL/PLGA multilayer formed at pH 7.4 to a solution at pH 1.5 or 13.5 leads to a strong reduction of its  $\beta$ -sheet content together with a partial or total dissociation of the polypeptide multilayer. A similar change in secondary structure on pH shift has been observed by Zhi and Haynie based on CD experiments. A substantial conformational change, from  $\beta$ -sheet to predominantly  $\alpha$ -helical structure, has been observed on contact of PLL/PLGA multilayers with strongly acidic ( $\text{pH} \leq 2.5$ ) or strongly basic ( $\text{pH} \geq 12.0$ ) solutions [36].

The secondary structural response of PLL/PLGA multilayers to a temperature rise (up to  $89^\circ\text{C}$ ) depends on the rate of temperature increase [55]. A slow temperature increase rate induces a reversible decrease of the  $\beta$ -sheet content at the expense of  $\alpha$ -helices. When the multilayer is heated rapidly, however, the  $\beta$ -sheet content increases, and a further increase is observed during the ensuing cooling process. Boulmedais et al. have proposed that the interactions between the amino groups of PLL and the carboxyl groups of PLGA favor a high temperature and lead to the formation of amide links [116]. The formation of such links between chains, even if their number is small, tends to stabilize the structure of the multilayer film. On the other hand, an increase in temperature tends to destabilize the film's secondary structures. Such a destabilization takes place, however, only when the chains can move freely with respect to each other. When the multilayer is heated slowly, the destabilization process happens before the formation of amide links. By contrast, when the multilayer is heated rapidly, some amide links may form before the  $\beta$ -sheets are destabilized. The relative freedom of movement of the chains gained by the temperature increase only allows the extension of the  $\beta$ -sheet domains, but it forbids their destruction (which would require larger movements). In the ensuing cooling process,  $\beta$ -sheets become even more stable, thus leading to a further increase of their content.

The above results have suggested that polypeptide multilayers may present significant secondary structures ( $\alpha$ -helix and  $\beta$ -sheet), and their structural stability may change in response to external stresses.

### 5.3. LBL Multilayers of Designed Polypeptides

The extreme flexibility in sequence design as well as the inclusion of specific biofunctional sequences enables great potential for the application and formation of multilayers from designed polypeptides.

In comparison with the large number of reports on the formation and uses of non-polypeptide polyelectrolyte multilayers, very few studies have been undertaken for the construction of multilayers from designed polypeptides [1, 2, 16, 30, 93, 98]. Strong polyions such as PSS, poly(vinyl sulfate) (PVS), poly(diallyldimethylammonium chloride) (PDDA), and PEI with a molecular weight (MW) between 50,000 and 100,000 have been used widely for the formation of polyelectrolyte multilayer films and microcapsules. These polyions contain hundreds of ionized groups in the range of pH 3–9. Similarly, PLL and PLGA contain hundreds of ionized groups at neutral pH. The influence of the polymerization degree on the formation of stable interpolyelectrolyte bulk complexes has been analyzed by Kabanov and Zezin [117, 118]. They have found that such complexes are stable when a polyion contains more than 20 charged groups in the sequence. However, complexes of our designed polypeptides [1, 2, 16, 30, 93, 98], which have approximately 16 charged groups, have also been found to be stable as described below. In our designed polypeptides, hydrogen bonding and hydrophobicity may also play an important role in the complex formation.

#### 5.3.1. Polypeptide Design

In general, polypeptide properties such as hydrophobicity, linear charge density, propensity to form secondary structure, and ability to form chemical cross-links can be varied by the design of the polypeptide sequence. Other polypeptide properties, including degree of dispersity and

**Table 2.** Examples of designed polypeptides for LBL multilayers.

Positively charged polypeptide		Negatively charged polypeptide	
P1	(KVKGKCKV) <sub>3</sub> KVKGKCKY	N1	(EVEGECEV) <sub>3</sub> EVEGECEY
P2	(KCKGKCKV) <sub>3</sub> KCKGKCKY	N2	(ECEGECEV) <sub>3</sub> ECEGECEY
P3	(KCKGKCKC) <sub>3</sub> KCKGKCKY	N3	(ECEGECEC) <sub>3</sub> ECEGECEY
P4	(QVSRRRRG) <sub>3</sub> QVSRRRRY	N4	(DQCEDEEG) <sub>3</sub> DQCEDEEY
P5	(KVKV) <sub>7</sub> KVKY	N5	(EVEV) <sub>7</sub> EVEY
P6	(KVKV) <sub>7</sub> KVKY	N6	(EVEN) <sub>7</sub> EVEY
P7	(KKKK) <sub>7</sub> KKKY	N7	(EEEE) <sub>7</sub> EEEEY
P8	(QVSRRRRG) <sub>5</sub> QVSRRRRY	N8	(DQCEDEEG) <sub>5</sub> DQCEDEEY

chemical modification of chain termini or side chains, can be controlled by selecting the method of synthesis or protocol. Due to recent advancements in methods of peptide synthesis, the number of possible, and, indeed, realizable polypeptide sequences is effectively unlimited.

Polypeptides have been designed for LBL of multilayers based on a highly interdisciplinary approach [105]. One main concern is that the electrostatic properties of the polypeptides must be compatible with the basic principle of LBL. A series of oppositely charged 32-mer and 48-mer polypeptides has been designed and tested extensively for LBL. Examples are given in Table 2, where K, E, V, G, C, D, Q, S, R, N, and Y represent, respectively, the amino acids lysine, glutamic acid, valine, glycine, cysteine, aspartic acid, glutamine, serine, arginine, asparagines, and tyrosine. Y is included for determination of the concentration of polypeptides in solution by absorbance at 274 nm. Cysteine is included in some of the polypeptides to show the ability to form chemical cross-linking. The net charge per unit length of these polypeptides is  $\geq 0.5$  at neutral pH, enabling self-assembly based on electrostatic attraction.

A polypeptide sequence could be designed on various principles, for instance, based on human genome information [105]. A highly interdisciplinary approach aimed at minimizing the immunogenicity of polypeptide multilayers has been developed. This approach is to base the amino-acid sequences on solvent-exposed regions in the folded states of proteins from the same organism. The approach may become more specifically tailored for intravenous applications by requiring an employed sequence to correspond to a known blood protein. In Table 2, the P4, N4, P8, and N8 sequences are designed using structural motifs that have been identified in the human genome [105].

Compared to proteins, polypeptides of low MW such as our designed 32-mers have advantages in purification and control over secondary structure before and after multilayer assembly. Moreover, the designed polypeptides allow exceptional control over assembly, and physical properties of the resulting multilayers can be tuned on the nanometer scale [1, 16]. On oxidation of the formed multilayers of cysteine-containing polypeptides, cysteine side chains reversibly form chemical cross-links between polymer chains [1, 2, 30, 93, 98]. By controlling the number, sequence, and type of polymer layers incorporated, it is possible to create a wide variety of chemically and structurally diverse polypeptide multilayers.

Two of our designed polypeptides, P1 and N1, have been used extensively as examples to illustrate the assembly and properties of multilayers made of designed polypeptides [1, 2, 16, 30, 93, 98]. Figure 6 shows the molecular models of P1 and N1 in extended conformation [2].

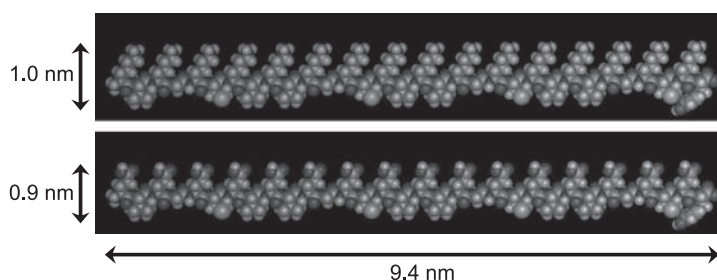


**Figure 6.** Molecular models of polypeptides P1 and N1. The hydrophilic side chains of lysine and glutamic acid are on the upper side and the hydrophobic side chains of valine, cysteine, and tyrosine are directed toward the bottom side of this model. The color scheme is as follows: carbon, green; nitrogen, blue; oxygen, red; hydrogen, white; sulfur, yellow. Reprinted with permission from [2], B. Li et al., *Biotechnol. Prog.* (ASAP article). © 2005, American Chemical Society.

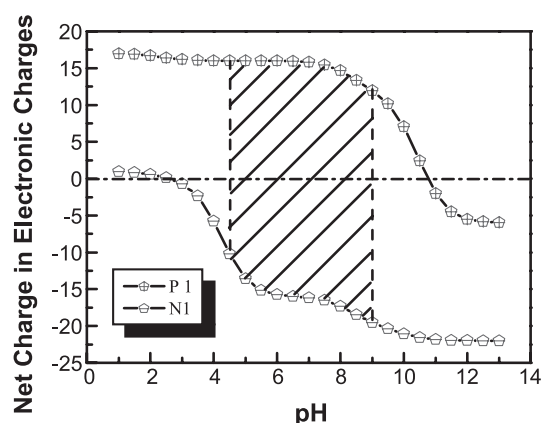


**Figure 7.** Influence of pH on calculated net charge of designed polypeptides, P1 and N1. The pH range 5–8 seems well suited to LBL. Reprinted with permission from [1], B. Li et al., *J. Nanosci. Nanotech.* 12, 2042 (2005). © 2005, American Scientific Publishers.

All hydrophobic side chains point in the same direction, all hydrophilic ones in the opposite direction. Both polypeptides have a contour length of  $\sim 9.4$  nm and a thickness of  $\sim 1.0$  nm. These two polypeptides are oppositely charged at pH 7.4; P1 is positive, whereas N1 is negative. The absolute charge density is  $\sim 0.5$  electronic charge per residue at pH 7.4. These two polypeptides bind to each other in a multilayer by electrostatic attraction. Other types of interaction, however, may also contribute to the multilayer assembly and secondary structure formation.

### 5.3.2. Property Control at Nanometer Scale of Multilayers Made of Designed Polypeptides

A variety of ways have been used to control the properties of LBL multilayers made of designed polypeptides.

**5.3.2.1. Tuning of Polypeptide Net Charge** Polypeptides are weak polyelectrolytes. A polypeptide will ordinarily be charged in an aqueous medium due to the presence of amino, carboxyl, guanidinium, or imidazole groups. Ionization or deionization in an aqueous solution changes the net charge of the molecule. For the LBL technique, it is necessary to know the net charge of the polypeptide molecules at the working pH. The desired charge of a designed polypeptide can be achieved not only by choice of amino acid composition, but also by adjustment of pH. The pH-dependence of the net charge of P1 and N1 has been calculated and shown in Figure 7 [1]. Each designed polypeptide has a relatively high charge per unit length at neutral pH. The net charge of these polypeptides changes with solution pH, and the pH range 5–8 is particularly well suited for LBL.

**5.3.2.2. Fine-Tuning of Materials Deposited** Figure 8 shows that polypeptides have been assembled on QCM quartz resonators [1]. The frequency shift has been converted to mass deposition. Continuous multilayer film growth has been observed, and the average mass change due to adsorption of a bilayer is  $\sim 380$  ng per cycle at 10 mM NaCl. Moreover, LBL assembly behavior of designed polypeptides depends on salt concentration. With increasing ionic strength, more material is adsorbed. The average mass deposition per bilayer is  $\sim 670$  ng at 100 mM NaCl, while it is  $\sim 290$  ng at 0 mM NaCl. The increase in adsorption with ionic strength is largely due to the charge screening, which decreases the repulsion between like-charged polypeptides. Therefore, the deposition of polypeptides can be simply controlled by varying ionic strength of the polypeptide solutions.

**5.3.2.3. Fine-Tuning of Film Thickness** Figure 9 shows that the thickness of polypeptide multilayers can be finely tuned simply by the number of layers [16]. The ellipsometry measurements, confirmed by surface profilometry measurements, have shown that the thickness of a

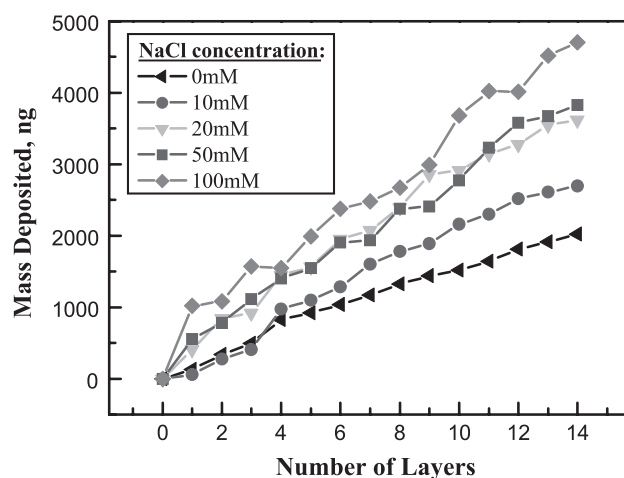


**Figure 8.** Adsorption of designed polypeptides (P1 and N1) as a function of ionic strength. Reprinted with permission from [1], B. Li et al., *J. Nanosci. Nanotech.* 12, 2042 (2005). © 2005, American Scientific Publishers.

polypeptide multilayer is  $\sim 1$  nm per layer at pH 7.4. The thickness increases with the number of adsorption steps and the film thickness can be tuned at the nanometer scale.

**5.3.2.4. Tuning of Film Density and Surface Morphology** Our recent experiments have shown that the solution pH can influence the density of polypeptide multilayers. pH substantially influences the assembly behavior of designed polypeptides [16]. Much more polymer is assembled at pH 7.4 than pH 7.8 or pH 8.9; about 2.6 times more materials are deposited at pH 7.4 compared to pH 8.9. Surprisingly, despite the apparent difference in deposited mass, the thickness, measured by both ellipsometry and surface profilometry, does not vary much for multilayers assembled at pH 7.4, 7.8, and 8.9 [16]. Therefore, the resulting films differ with regard to density. This marked difference in film density in the 1.5 unit pH range is believed to be related to the charge mismatch at these pH values; charge density depends on pH. Also, the surface morphology of these polypeptide multilayers greatly varies [16]. Figure 10 shows the AFM images of the surface morphology of 20 bilayer polypeptide multilayers. The multilayer prepared at pH 7.4 is relatively smooth [Figure 10c], whereas the one assembled at pH 8.9 is comparatively rough [Figure 10a]. The multilayer fabricated at pH 7.8 has an intermediate roughness [Figure 10b]. The same result has been obtained with independently made 10 bilayer polypeptide multilayers.

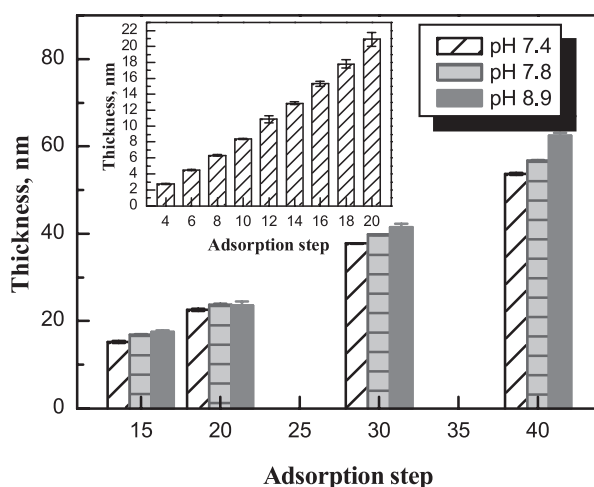


**Figure 9.** Multilayer nanofilms made of designed polypeptides P1 and N1 vs. adsorption steps. Reprinted with permission from [16], Y. Zhong et al., *Biotechnol. Prog.* (ASAP article). © 2005, American Chemical Society.



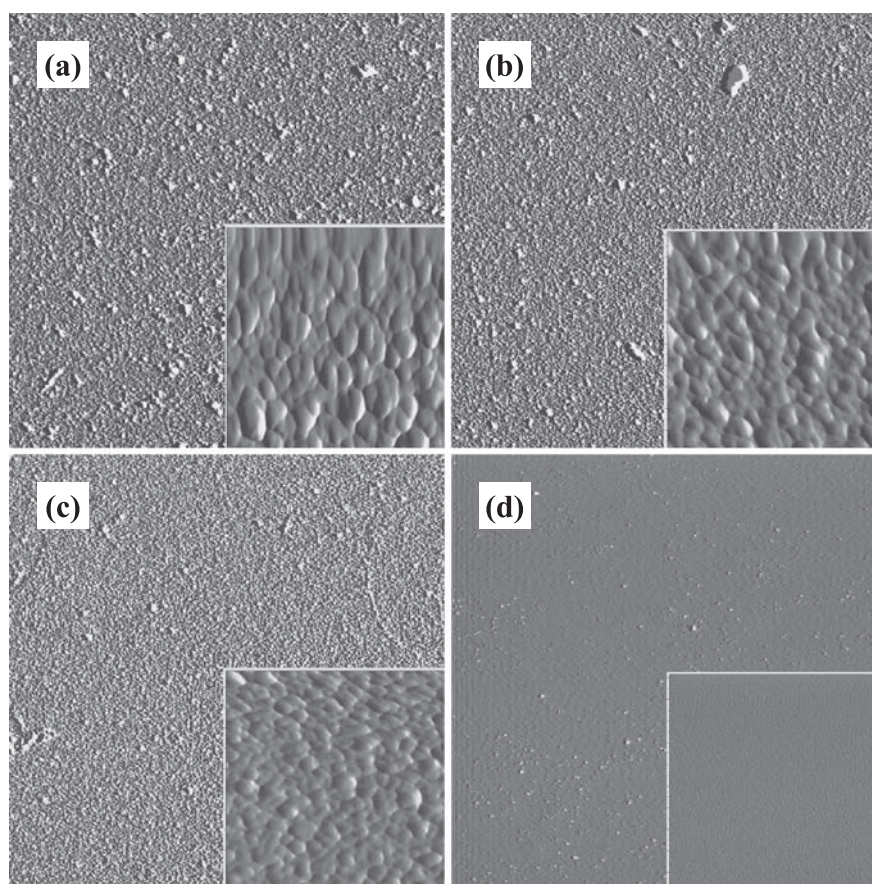


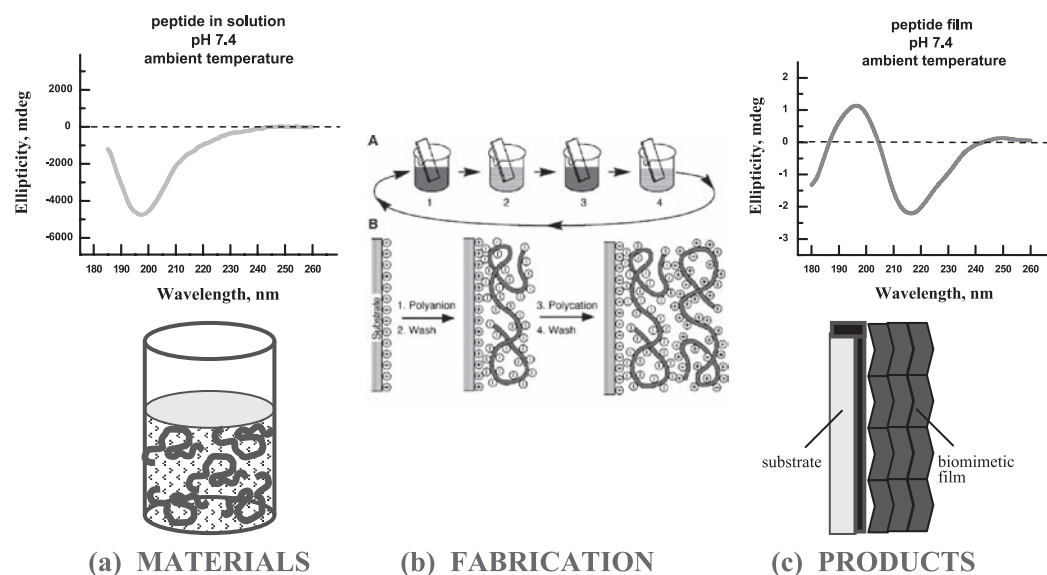
**Figure 10.** AFM micrographs of 20-bilayer polypeptide films deposited at different pH values,  $20\ \mu\text{m} \times 20\ \mu\text{m}$  and  $1\ \mu\text{m} \times 1\ \mu\text{m}$  (insets). (a) pH 8.9, (b) pH 7.8, (c) pH 7.4, and (d) Si wafer. Vertical scales for  $20\ \mu\text{m} \times 20\ \mu\text{m}$  are 194 nm, 150 nm, 84 nm, 36 nm, respectively; and for  $1\ \mu\text{m} \times 1\ \mu\text{m}$  are 34 nm, 29 nm, 27 nm, 15 nm, respectively. Reprinted with permission from [16], Y. Zhong et al., *Biotechnol. Prog.* (ASAP article). © 2005, American Chemical Society.

### 5.3.3. Unique Properties of Multilayer Films Made of Designed Polypeptides

**5.3.3.1. Secondary Structure** Non-polypeptide polyelectrolyte multilayers do not show well-ordered structures, while polypeptide multilayers display certain secondary structures, e.g.,  $\alpha$ -helix [3] and  $\beta$ -sheet [1, 2].

Boulmedais et al. and Arys et al. have reported that the secondary structure of PLL/PLGA multilayers should be very close to the structure of the polyanion/polycation complexes in solution [9, 115]. They believed that the constraints imposed by the presence of the substrate surface should have only marginal effects on the secondary structure of the multilayer. By contrast, the secondary structure of multilayers made of our designed polypeptides is significantly different from that of their corresponding complexes in solution [Scheme 5]: predominant  $\beta$ -sheet in multilayers while random coil in solution complex. This may relate to the unique structure of the designed polypeptides.

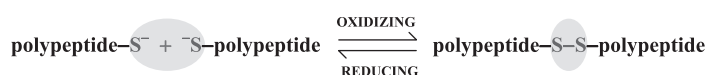
Scheme 5 shows a schematic diagram of polypeptide multilayer assembly of designed polypeptides P1 and N1. Prior to assembly, P1, N1, and their complex are in a random coil conformation in solution [Scheme 5a]. LBL of these polypeptides is self-limiting [Scheme 5b], according to quartz crystal microbalance measurements. The adsorption is driven by electrostatic attraction between the oppositely charged polypeptides, while it is limited by electrostatic repulsion between the same-charged polypeptide molecules. After self-assembly, the adsorbed polypeptides adopt predominant  $\beta$ -sheet structure [Scheme 5c].



**Scheme 5.** Schematic diagram of polypeptide multilayer film assembly by LBL. The polypeptides undergo a conformational change from random coil in solution (a) to  $\beta$  sheet on incorporation into the film (c) upon LBL (b).

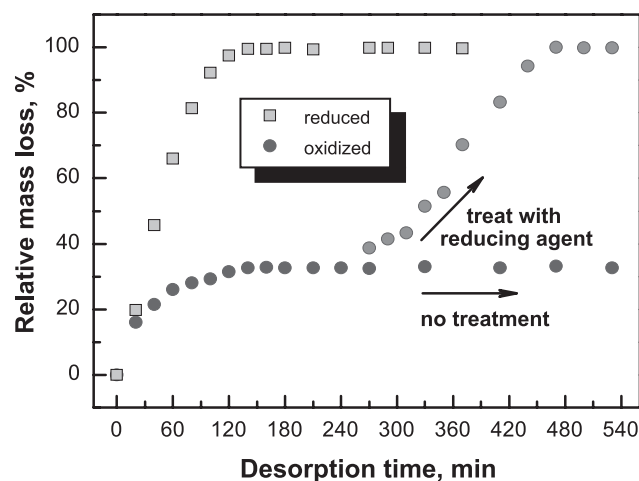
**5.3.3.2. “Natural” and Reversible Film Cross-Linking** Polypeptide multilayers, similar to other polyelectrolyte ones, may disintegrate at strong acidic or basic environments [30]. Fortunately, a polypeptide-inherent reversible cross-linking method can be introduced. Polypeptides can be cross-linked by disulfide bonding, enabling the formation of polypeptide networks or gels and strengthening multilayer film structure [1, 2, 30, 93]. Control over polypeptide design and synthesis enables inclusion of the amino acid cysteine, as shown in P1, P2, P3, N1, N2, and N3. On oxidation, two cysteine residues can form a disulfide bond [Scheme 6]. This results in covalent stabilization of the polypeptide multilayer and substantially enhances the stability of the multilayer [1, 2, 30, 93].

Figure 11 shows that disulfide cross-link formation increases film stability against chemical degradation, substantially reducing the kinetics and extent of disintegration of an oxidized polypeptide film relative to a non-oxidized one [30]. Moreover, disulfide bond formation in a polypeptide film can be reversed by treatment with a reducing agent. QCM has been used to measure the effectiveness of cross-linking by treating the samples at pH 2.0 [30]. Two sets of samples are assembled, one set is oxidized and the other is not. Figure 11 shows that acidic treatment of non-oxidized samples leads to multilayer dissociation with relatively rapid kinetics. By contrast, oxidized polypeptide multilayer samples retain most of their mass at an acidic pH. All the retained material is lost from the oxidized samples at pH 2.0. However, treatment of the samples by immersion in a reducing aqueous environment, thereby reducing the disulfide bonds in the oxidized samples, leads to complete multilayer dissociation at an acidic pH as in the non-oxidized samples. This resembles the known reversibility of disulfide bond formation in proteins. The mechanism of this process is illustrated in Scheme 7. Exposure of a cysteine-containing film to an oxidizing solution promotes disulfide bond formation. Cross-links form between like-charged polypeptides within a single layer and between oppositely charged polypeptides in adjacent layers [Scheme 7]. The product is a cross-linked multilayer of three-dimensional structure that resists dissociation in an acidic environment. By contrast, non-cross-linked (i.e., reduced) samples readily dissociate under these conditions due to charge repulsion between positively charged polypeptides. By treating the disulfide bonds with reducing agents such as dithiothreitol, they are reversed to free thiol groups and the multilayer starts to disintegrate at extreme conditions. The approach mimics the



**Scheme 6.** Chemical cross-link, i.e., disulfide bonds, formation, and locking mechanisms for cysteine-containing polypeptides. The formation is reversible upon reducing. The disulfide bond is shown in red.

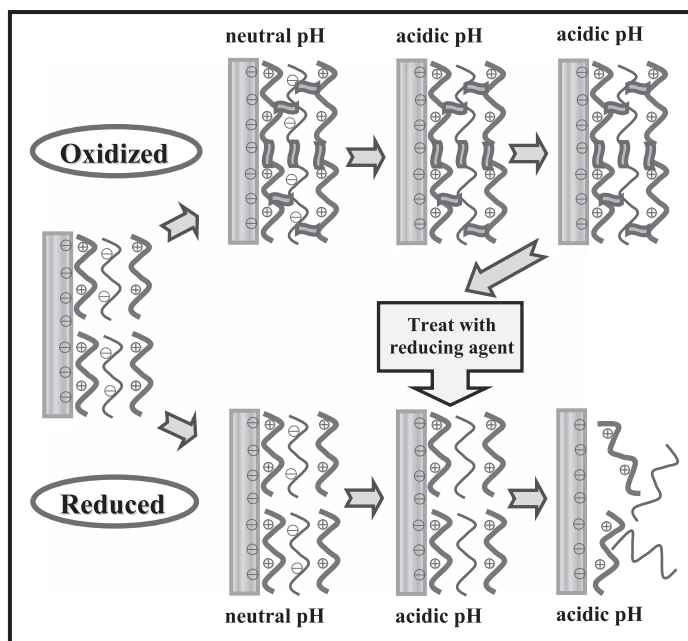




**Figure 11.** Stability test at pH 2.0 of a cysteine-containing polypeptide film (P1 and N1), monitored by quartz crystal microbalance. A representative time course of loss of polypeptide from the film is shown. After treatment with a reducing agent at an acidic pH, complete disassembly of the previously cross-linked film is observed. Disulfide bond formation is reversible. Reprinted with permission from [30], B. Li and D. T. Haynie, *Biomacromolecules* 5, 1667 (2004). © 2004, American Chemical Society.

known stabilization by disulfide bonds of secreted hormones and proteins, for instance, insulin and lysozyme. The reversibility of disulfide bond formation is important in the metabolism of insulin—the two chains undergo rapid proteolysis following reduction by glutathione-insulin transdehydrogenase and other bioactive polypeptides and proteins.

The extent of cross-linking can be controlled by optimizing the oxidizing process [1] and by changing the number of cysteine residues per unit length in the polypeptide design. Three sets of polypeptides with varying cysteine residues have been designed: 4 cysteines for P1 and N1, 8



**Scheme 7.** Effect of disulfide bond formation on cysteine-containing polypeptide multilayer stability under extreme conditions, in this case, strong acid. Disulfide cross-links stabilize the oxidized film. The formation of disulfide bonds is reversible. Upon the addition of a reducing agent, the disulfide-bonded multilayer becomes unstable at an acidic pH. Counterions are omitted for clarity. Reprinted with permission from [30], B. Li and D. T. Haynie, *Biomacromolecules* 5, 1667 (2004). © 2004, American Chemical Society.

cysteines for P2 and N2, and 11 cysteines for P3 and N3. We have found that disulfide cross-linked polypeptide films made of P1 and N1 lose about 30% of mass [Figure 11] in acidic conditions, though no obvious mass loss has been observed in polypeptide films made of P2 and N2. This enables further control of the stability of polypeptide multilayers.

Other researchers have cross-linked polyelectrolyte multilayer films by thermal or photoinduced processes for various purposes, e.g., to micropattern polymer films, to stabilize enzyme crystals for synthetic applications, to enhance ion-transport selectivity of polyelectrolyte membranes, to covalently attach multilayers upon UV irradiation, and to stabilize biocompatible albumin/heparin coatings [58, 119–123]. In all such cases, however, cross-linking is irreversible. Disulfide bond cross-linking of polypeptide films is distinguished by chemical reversibility. This suggests the possibility of environmental triggering of increased or decreased film stability. The extracellular environment is oxidizing, while the intracellular one is reducing. Moreover, disulfide bonds can be formed simply by exposing thiol to air; the addition of chemicals is not required. The disulfide cross-linking approach is potentially useful for controlling the stability of various polypeptide-based technologies, e.g., biocompatible coatings for implanted devices, food coatings, and microcapsules and artificial cells [93].

**5.3.3.3. Structural Stability under Various External Stresses** By introducing disulfide cross-linking, multilayers made of designed polypeptides are stable under a variety of external stresses such as pH jumps, temperature increases and decreases, exposure to organic solvents, and changes in the nature of the outer layers of the multilayer [1, 2, 30, 93, 98]. We have shown that cross-linked multilayers made of designed cysteine-containing polypeptides are substantially more stable in a strong acid or base than when the polypeptide multilayer is stabilized by electrostatic interaction alone [2]. P1/N1 multilayers, regardless of cross-linking, are very stable in organic solvents and, when dried, at extreme temperatures (e.g., freezing to  $-196^{\circ}\text{C}$  for 10 min or heating to  $100^{\circ}\text{C}$  for 1 h); film structure is preserved because no structural change has been observed by optical spectroscopy [2]. This is in marked contrast to the behavior of proteins, which tend to denature under comparable conditions. Cross-linking by oxidation of cysteine, though useful, is not necessary for preparing a stable polypeptide multilayer film.

We have also studied the perturbation of the polypeptide multilayer structure by deposition of PAH and PSS on the multilayer surface [98]. We have revealed differences in behavior attributable to physical properties of the polypeptides. It seems that PAH and PSS chains would diffuse into PLL/PLGA multilayers, resulting in rearrangement of polymer chains and/or replacement of PLGA by PSS. There is some induction of  $\alpha$ -helical structure in PLL/PLGA multilayers on deposition of PAH and PSS. By contrast, multilayers built of designed polypeptides resist perturbation by deposition of PAH and PSS. The amount of adsorbed material and the secondary structure content of P1/N1 multilayers remain almost unchanged on deposition of the non-polypeptide polymers, regardless of chemical cross-linking. The apparent reason is that the designed polypeptides are much smaller and more hydrophobic than PLL and PLGA, and, therefore, assemble into denser and more stable multilayers. Control of polypeptide structure allows control over polypeptide multilayer properties.

In summary, we have explored the design of polypeptides with various properties, and these polypeptides have been successfully used for the preparation of multilayer films. The properties of polypeptides can be tuned by pH and other influences. The properties of the films can be easily tuned by polypeptide design, assembly conditions, cross-linking, and so on. Therefore, polypeptide multilayers with varying properties could be achieved by polypeptide design, control of the self-assembly process, and post-preparation treatment.

#### **5.4. Multilayers Consisting of One Polypeptide and One Non-Polypeptide Component**

Polypeptides have also been used together with non-polypeptide polyelectrolytes to develop multilayers of ordered structures. Cooper et al. have prepared polypeptide-dye multilayers using LBL [51]. PLL and anionic dyes such as Congo Red and copper phthalocyanine tetrasulfonic acid have been used. Evidence for induced ordering of the dye by the polypeptide matrix has been obtained from circular and linear dichroism measurements. FTIR spectra have shown that the multilayer is in an  $\alpha$ -helical conformation. A high  $\alpha$ -helix content has also been observed in PLGA/PAH multilayers at pH 7.4, while PLGA itself in solution is mainly in a random coil conformation [88]. The mass and thickness of PLGA/PAH multilayers increase exponentially with the number of layers.

Müller et al. have developed PLGA/PDDA and PLL/PVS multilayers [96]. An increase of order has been observed with decreasing polyelectrolyte concentration in the PLGA/PDDA multilayer and with an increasing number of layers in the PLL/PVS multilayer.

### 5.5. Polypeptide Microcapsules

Polymer microcapsules are an important class of functional materials widely used in encapsulation, separation, and biological applications [124]. Microcapsules of polypeptides are of particular interest because of their intrinsic compatibility with biomolecules, high biodegradability, and certain functions that can be endowed by designing suitable primary (and secondary) structures. In spite of these promising features, there have been only a few studies on self-assembly of polypeptide microcapsules [93, 125–127]. Polypeptide microcapsules have been prepared by Morikawa et al. [125] from simple polypeptides, e.g., poly( $\gamma$ -benzyl L-glutamate), with well-defined structures. Kidchob et al. have developed polypeptide microcapsules that show pH-responsive release of encapsulated dextran [126]. Wang et al. have prepared and studied polypeptide microcapsules as drug carriers [127].

We have developed microcapsules with controllable stability using designed cysteine-containing polypeptides [93]. Figure 12 displays the confocal scanning micrographs of polypeptide microcapsules. The images show spherical films of P1 and N1 before and after dissolution of the template cores. The LBL assembly process developed for macroscopic planar surfaces was adapted to colloidal particles, e.g., melamine formaldehyde (latex) particles, for the preparation of microcapsules [128, 129]. A polycation solution is added to a suspension of charged particles; following saturation of polymer adsorption, the particles are separated from free polycations in solution usually by means of centrifugation. Then a polyanion layer is deposited in the same way. This whole process can be repeated, and the template particle can be dissociated to form empty microcapsules.

Similar to multilayer films made of cysteine-containing polypeptides, the stability of P1/N1 microcapsules can also be substantially enhanced upon oxidation to form disulfide bonds [93]. Polypeptide layers are cross-linked by oxidation, forming disulfide-bond-“locked” microcapsules. This process stabilizes the capsules in “harsh” environments. Disulfide bond formation in these polypeptide microcapsules is reversible.

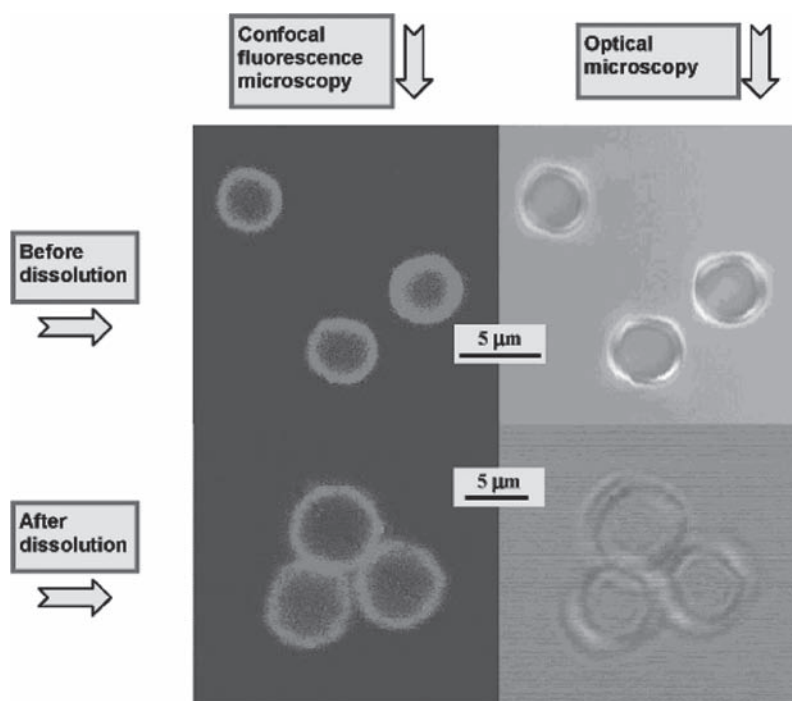


**Figure 12.** Confocal scanning micrographs of polypeptide microcapsules. The images show spherical films of polypeptides (P1 and N1) before and after dissolution of the particle cores. Reprinted with permission from [93], D. T. Haynie et al. *Langmuir* 21, 1136 (2005). © 2005, American Chemical Society.

## 6. APPLICATIONS OF POLYPEPTIDE MULTILAYERS

In general, polyelectrolyte multilayers can be used as biosensors, nanoreactors, drug delivery systems, and so on [17]. The biocompatibility, biofunctionality, and immunogenicity of polypeptides will be more favorable for biomedical applications of LBL structures than those made from non-polypeptide polyelectrolytes, for instance, PAH and PSS, particularly if the sequences are based on genomic information [105]. Applications of polypeptide multilayers are very promising in a variety of areas including membranes for ion separation, drug delivery, artificial cells, cardiovascular applications, multifunctional molecular coatings, biosensors, nanoreactors, liquid/liquid electrochemical interfaces, and so on. Following are a few examples.

### 6.1. Chiral Separation

The enantioselectivity of chiral compounds is of great importance to the pharmaceutical industry. Enantiomers are considered distinctly different compounds because enantiomers of drug substances may have distinct biological interactions, and, consequently, profoundly different pharmacological, pharmacokinetic, or toxicological activities [130]. It is clear that chiral drugs should be enantio-separated and that each enantiomer should be used separately [131]. Therefore, the development of suitable methods for the enantio-separation of chiral drugs is important. The use of polypeptides has advantages because these systems mimic the biomembranes in the human body. Polypeptides, optically active, have been used to build multilayers as an alternative method of chiral drug separation [83, 132]. Rmaile and Schlenoff have developed polypeptide multilayers consisting of poly(D-lysine) and poly(D-glutamic acid), i.e., PDL/PDGA, for chiral recognition of ascorbic acid in open-tubular capillary electrochromatography [83]. Their work has illustrated remarkable permeability and chiral selectivity [Figure 13]. Kamande et al. have reported the use of a multilayer coating that consists of PLL and the polymeric dipeptide surfactant poly(sodium undecanoyl-L-leucyl-alaninate) for the chiral separation of three binaphthyl derivatives and two  $\beta$ -blockers [132]. They have shown that the presence of NaCl in each of the polyelectrolytes plays a significant role in the chiral selectivity of the polypeptide multilayer coating. The separation efficiency and resolution of enantiomers vary with the number of layers. The separation of BNP enantiomers and labetalol diastereoisomers results in high peak efficiencies, and run-to-run and capillary-to-capillary reproducibility is very good. The coating is stable and allows for more than 290 runs to be performed in the same capillary.

### 6.2. Anti-Inflammatory Coatings

Polyelectrolyte multilayers are excellent vehicles for incorporating a wide variety of additives such as antioxidants, antifungal agents, antimicrobials, colors, and nutrients. Several researchers have demonstrated that antimicrobial compounds can be added to polyelectrolyte films to reduce microbial loads for various applications.

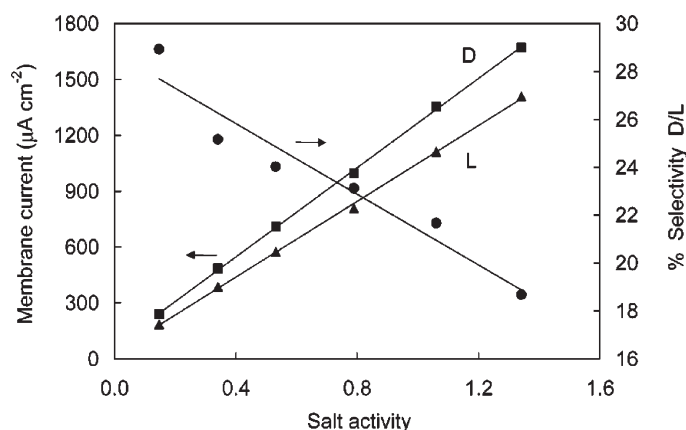


**Figure 13.** Left y-axis shows membrane current density for two enantiomeric forms of ascorbic acid. Polyelectrolyte multilayer is 16 alternating layers of PDL and PDGA. Right y-axis shows the percent selectivities of D- over L-ascorbic acid as a function of supporting salt concentration. Solution included 10 mM phosphate (pH 7.4). Voltage = 900 mV. Reprinted with permission from [83], H. H. Rmaile and J. B. Schlenoff, *J. Am. Chem. Soc.* 125, 6602 (2003). © 2003, American Chemical Society.

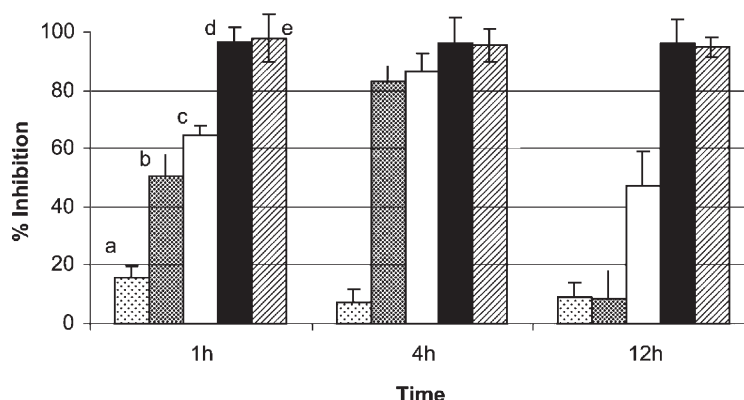


**Figure 14.** Inhibition of TNF $\alpha$  secretion by THP-1 cells, incubated with 10 ng mL<sup>-1</sup> of LPS, grown on multilayered films containing cCD-Px complexes. Cells are deposited on the multilayered films: (a) PEI-(PLGA-PLL)<sub>6</sub>-Px, (b) PEI-(PLGA-PLL)<sub>6</sub>-cCD-Px, (c) PEI-(PLGA-PLL)<sub>6</sub>-cCD-Px-PLL-(PLGA-PLL)<sub>3</sub>, (e) PEI-(PLGA-PLL-cCD-Px)<sub>3</sub>-PLL, built in 24-well plates at a density of  $5 \times 10^5$  cells/well. After 1, 4, or 12 h incubation, cells are centrifuged and total TNF $\alpha$  levels are measured. The results are the means of three measurements, and the vertical bars correspond to the standard error. Reprinted with permission from [87], N. Benkirane-Jessel et al., *Adv. Funct. Mater.* 14, 174 (2004). © 2004, John Wiley & Sons, Inc.

Benkirane-Jessel et al. have developed PLL/PLGA multilayers as potential systems for biomaterials coatings with local anti-inflammatory drug delivery systems [87]. Piroxicam (Px), in the form of complexes with a charged 6<sup>A</sup>-carboxymethylthio- $\beta$ -cyclodextrin (cCD), has been incorporated in the polypeptide multilayer and used as an anti-inflammatory agent. The structure of cCD-Px complexes in the polypeptide multilayers has been studied by Fourier transform Raman spectroscopy. The anti-inflammatory properties of the cCD-Px complexes in the polypeptide multilayers have been investigated by determining the inhibition of pro-inflammatory TNF $\alpha$  production by monocytic cells stimulated by lipopolysaccharide (LPS). It has been shown that the cCD-Px functionalized polypeptide multilayers act as active coatings to control inflammation. Moreover, the anti-inflammatory activity over time can be tuned by controlling the architecture of the polypeptide multilayers [Figure 14]. The cell may come in contact with the embedded active biological molecules through local film degradation, or it is possible that slow cCD-Px diffusion through the multilayer could continue to activate the adhering cells. Such modularly functionalized coatings may, in the future, become potent tools for the modification of biomaterial surfaces as applied to implants, prostheses, or in tissue engineering. The results highlight the potential for incorporating antimicrobial compounds into polypeptide multilayers. These materials can be used for controlling spoilage, enhancing shelf life, and improving the microbial safety of food and drug carriers.

### 6.3. Polypeptide Multilayers as Electrochemical Interfaces for Ion and Electron Transport

By incorporating electroactive ions inside, polypeptide multilayers can serve as an electrochemical interface for ion and electron transport [53]. Cheng and Corn have developed PLL/PLGA ultrathin polypeptide multilayers on alkanethiol-modified gold electrodes. By immersion of the polypeptide multilayers into a solution of ferri/ferrocyanide ions, the electroactive ions have been incorporated into the polypeptide multilayers. The majority of the ions have been found to be incorporated in the bulk of the film rather than just the outermost layer. The ferri/ferrocyanide ions in the multilayer can be reversibly reduced and oxidized without any loss of ferri/ferrocyanide ions to the surrounding organic solvent such as 1,2-dichloroethane. These polypeptide multilayers can be used to study both ion and electron transport across the film/1,2-dichloroethane interface. As further demonstrated by Hoffmannová et al. [54], the transport of the ferri/ferrocyanide in the polypeptide multilayer film is the rate limiting step of the electron transfer process. The diffusion coefficient of the ferri/ferrocyanide is on the order of  $10^{-11}$ – $10^{-12}$  cm<sup>2</sup> s<sup>-1</sup>, and the biomolecular rate constant of the electron transfer reaction is 0.2 cm s<sup>-1</sup> M<sup>-1</sup>, which is in good agreement with data published in the literature on similar systems.



#### 6.4. Polypeptide Multilayers in Nanofiltration for Ion Separation

Polypeptide multilayers have been deposited in microporous membranes for ion separation [133]. The deposition of PLL/PLGA multilayers within confined pore geometries in microporous membranes leads to an enhanced volume density of ionizable groups in the membrane phase. This increase in the effective charge density allows for Donnan or charge-based exclusion of ionic species (especially divalent co-ions) using microporous materials characterized by permeability values that exceed conventional membrane processes. The properties of the resulting materials have been found to depend highly on the ionic strength of the carrier solvent used for the multilayer deposition. Compared to assemblies in the absence of salt, the multilayer membranes assembled at high salt concentration display lower pure water permeability and enhanced overall adsorption. This is because in the deposition process, the number of ionic site interactions per adsorbed chain is smaller at high salt concentration than at low salt concentration. Thus, larger segments of the adsorbing polymer extend into the pore cross-section at high salt concentration and lead to greater solvent resistance. In addition, an excess of these charged constituents away from the pore assembly facilitates ion exclusion in open membrane materials. Multilayer assemblies prepared at high ionic strength, e.g., 0.5 M NaCl solution, provide excellent separation of divalent co-ions, even in the ultradilute regime. This work and other recent work on non-polypeptide polyelectrolytes [119, 134–138] have shown great promise in nanofiltration and reverse osmosis applications.

AQ2

As aforementioned, great efforts have been made to explore the applications of polypeptide multilayers over the past years. Multilayers made of designed polypeptides could have a broader range of application because polypeptide design may enable a great degree of control over bioactive properties in defined and “natural” ways. Certain functional polypeptide sequences, for instance, sequences from extracellular and matricellular proteins that contain the Arg-Gly-Asp (RGD) cell adhesive sequence, could be incorporated into the designed polypeptide sequence. This RGD motif is responsible for integrin-mediated cell adhesion and has been found in fibronectin and many other extracellular matrix and matricellular proteins. The RGD motif has been included in streptavidin widely utilized proteins, and its incorporation has facilitated cell adhesion [139]. This RGD sequence could be inserted into our designed polypeptide sequences to make these polypeptide multilayers possess a cell-adhesion property. Also, sequences having antimicrobial properties could be easily included when designing polypeptide sequences.

### 7. CONCLUSIONS AND FUTURE PROSPECTS

This chapter has described the development and fabrication as well as the applications of polypeptide multilayer films and microcapsules. Polypeptide multilayers are prepared by two main methods, i.e., LBL and LB.

Increasing activity in the field of polypeptide multilayer films and microcapsules is due to several factors. First, the application of the technique, i.e., LBL, allows one to easily deposit films and microcapsules containing polypeptides and/or other biomacromolecules. LBL also allows one to deposit multilayers and to form complex structures with controlled assembly behavior and multilayer properties. Second, polypeptides can now be chemically synthesized or recombinantly made in cells or plants with little difficulty due to the advancement in the past decades of chemical synthesis methods of biopolymers and biotechnology. Third, there is flexibility and diversity in designing polypeptides; polypeptides with specific biofunctionalities and structures can be obtained, and polypeptide design offers the possibility of a reversible “polypeptide-inherent” cross-linking method. Therefore, the future of polypeptide multilayers, especially those of designed polypeptides, looks extremely promising as we continue to find novel applications for these advanced materials. We have explored the design of 32-mer polypeptides for LBL of multilayer films and microcapsules. New developments may include the design of polypeptides with specific biofunctionalities such as including an RGD sequence for “bio-active” coatings that can be used to promote the adhesion of cells.

### ACKNOWLEDGMENTS

The support from the Department of Orthopedics, the School of Medicine, WVNano, and WVU Research Corporation, at West Virginia University is gratefully acknowledged. I would thank Suzanne Smith for proofreading the manuscript and assisting with the figures.



## REFERENCES

1. B. Li, D. T. Haynie, N. Palath, and D. Janisch, *J. Nanosci. Nanotech.* 12, 2042 (2005).
2. B. Li, J. Rozas, and D. T. Haynie, *Biotechnol. Prog.* (In press).
3. M. Müller, T. Reihs, B. Kebler, H. J. Adler, and K. Lunkwitz, *Macromol. Symp.* 211, 217 (2004).
4. T. Jaworek, D. Neher, G. Wegner, R. H. Wieringa, and A. J. Schouten, *Science* 279, 57 (1998).
5. L. Hartmann, T. Kratzmuller, H. G. Braun, and F. Kremer, *Macromol. Rapid Commun.* 21, 814 (2000).
6. T. Strother, W. Cai, X. Zhao, R. J. Hamers, and L. M. Smith, *J. Am. Chem. Soc.* 122, 1205 (2000).
7. C. Picart, P. Lavalle, P. Hubert, F. J. G. Cuisinier, G. Decher, P. Schaaf, and J. C. Voegel, *Langmuir* 17, 7414 (2001).
8. P. Lavalle, C. Gergely, F. J. G. Cuisinier, G. Decher, P. Schaaf, and J. C. Voegel, *Macromolecules* 35, 4458 (2002).
9. F. Boulmedais, P. Schwinte, C. Gergely, J. C. Voegel, and P. Schaaf, *Langmuir* 18, 4523 (2002).
10. P. Schwinte, J. C. Voegel, C. Picart, Y. Haikel, P. Schaaf, and B. Szalontai, *J. Phys. Chem. B* 105, 11906 (2001).
11. J. Chluba, J. C. Voegel, G. Decher, P. Erbacher, P. Schaaf, and J. Ogier, *Biomacromolecules* 2, 800 (2001).
12. P. Schwinte, V. Ball, B. Szalontai, Y. Haikel, J. C. Voegel, and P. Schaaf, *Biomacromolecules* 3, 1135 (2002).
13. L. Richert, Ph. Lavalle, D. Vautier, B. Senger, J. F. Stoltz, P. Schaaf, J. C. Voegel, and C. Picart, *Biomacromolecules* 3, 1170 (2002).
14. R. K. Iler, *J. Colloid Interface Sci.* 21, 569 (1966).
15. G. Decher, *Science* 277, 1232 (1997).
16. Y. Zhong, B. Li, and D. T. Haynie, *Biotechnol. Prog.* (In press).
17. Y. Lvov, in *Protein Architecture, Interfacial Molecular Assembly and Immobilization Biotechnology*, Y. Lvov and H. Möhwald, Eds., Marcel Dekker, New York (2000), p. 125.
18. J. F. Rusling, in *Protein Architecture: Interfacial Molecular Assembly and Immobilization Biotechnology*, Y. Lvov and H. Möhwald, Eds., Marcel Dekker, New York (2000), p. 337.
19. V. Erokhin, in *Protein Architecture: Interfacial Molecular Assembly and Immobilization Biotechnology*, Y. Lvov and H. Möhwald, Eds., Marcel Dekker, New York (2000), p. 99.
20. J. C. Cheftel, J. L. Cuq, and D. Lorient, in *Food Chemistry*, O. R. Fennema, Ed., Marcel Dekker, New York (1985), p. 245.
21. I. D. Campbell and R. A. Dwek, *Biological Spectroscopy*, Benjamin/Cummings, CA (1984).
22. C. S. Winter and R. H. Tredgold, *Thin Solid Films* 123, L1 (1985).
23. M. Rikukawa, K. Sanui, and N. Ogata, *Synth. Met.* 84, 393 (1997).
24. T. M. Cooper, A. L. Campbell, C. Noffsinger, J. Gunther-Greer, R. L. Crane, and W. Adams, *Mater. Res. Soc. Symp. Proc.* 351, 239 (1994).
25. T. E. Creighton, *Proteins: Structures and Molecular Properties*. 2nd ed., Freeman, New York (1993), p. 287.
26. A. Gennadios, *Protein-based Films and Coatings*, CRC Press, Boca Raton, FL (2002), p. 1.
27. K. B. Blodgett, *J. Am. Chem. Soc.* 57, 1007 (1935).
28. B. P. Binks, *Adv. Colloid Interface Sci.* 34, 343 (1991).
29. O. N. Oliveira, Jr., J. A. He, V. Zucolotto, S. Balasubramanian, L. Li, H. S. Nalwa, J. Kumar, and S. K. Tripathy, in *Handbook of Polyelectrolytes and Their Applications*, S. K. Tripathy, J. Kumar, and H. S. Nalwa, Eds., American Scientific Publishers, Stevenson Ranch, CA (2002), Vol. 1, p. 1.
30. B. Li and D. T. Haynie, *Biomacromolecules* 5, 1667 (2004).
31. S. A. Sukhishvili and S. Granick, *J. Am. Chem. Soc.* 122, 9550 (2002).
32. C. Schüler and F. Caruso, *Biomacromolecules* 2, 921 (2001).
33. A. J. Chung and M. F. Rubner, *Langmuir* 18, 1176 (2002).
34. J. A. Hiller and M. F. Rubner, *Macromolecules* 36, 4078 (2003).
35. K. C. Wood, J. Q. Boedicker, D. M. Lynn, and P. T. Hammond, *Langmuir* 21, 1603 (2005).
36. Z. L. Zhi and D. T. Haynie, *Macromolecules* 37, 8668 (2004).
37. G. B. Sukhorukov, M. Brumen, E. Donath, and H. Möhwald, *J. Phys. Chem. B* 103, 6434 (1999).
38. A. A. Antipov, G. B. Sukhorukov, E. Donath, and H. Möhwald, *J. Phys. Chem. B* 105, 2281 (2001).
39. M. K. Park, S. Deng, and R. C. Advincula, *Langmuir* 21, 5272 (2005).
40. O. P. Tiourina, A. A. Antipov, G. B. Sukhorukov, N. L. Larionova, Y. Lvov, and H. Möhwald, *Macromol. Biosci.* 1, 209 (2001).
41. A. J. Khopade and F. Caruso, *Biomacromolecules* 3, 1154 (2002).
42. R. V. Klitzing and H. Möhwald, *Macromolecules* 29, 6901 (1996).
43. A. Wu, D. Yoo, J. K. Lee, and M. F. Rubner, *J. Am. Chem. Soc.* 121, 4883 (1999).
44. A. C. Fou, O. Onitsuka, M. Ferreira, M. F. Rubner, and B. R. Hsieh, *J. Appl. Phys.* 79, 7501 (1996).
45. W. Kong, X. Zhang, M. Gao, H. Zhou, W. Li, and J. Shen, *Macromol. Rapid Commun.* 15, 405 (1994).
46. Y. Lvov, H. Haas, G. Decher, H. Möhwald, A. Michailov, B. Mtchedlishvily, E. Morgunova, and B. Vainshtain, *Langmuir* 10, 4232 (1994).
47. Y. Lvov, K. Ariga, and T. Kunitake, *J. Am. Chem. Soc.* 117, 6117 (1995).
48. F. Caruso, D. N. Furlong, K. Ariga, I. Ichinose, and T. Kunitake, *Langmuir* 14, 4559 (1998).
49. A. Kotov, I. Dékány, and J. H. Fendler, *J. Phys. Chem.* 99, 13065 (1995).
50. Y. Lvov, K. Ariga, I. Ichinose, and T. Kunitake, *Langmuir* 12, 3038 (1996).
51. T. M. Cooper, A. L. Campbell, and R. L. Crane, *Langmuir* 11, 2713 (1995).
52. K. Ariga, Y. Lvov, and T. Kunitake, *J. Am. Chem. Soc.* 119, 2224 (1997).

53. Y. Cheng and R. M. Corn, *J. Phys. Chem. B* 103, 8726 (1999).
54. H. Hoffmannová, D. Fermin, and P. Krtíl, *J. Electroanal. Chem.* 562, 261 (2004).
55. F. Boulmedais, M. Bozonnet, P. Schwinte, J. C. Voegel, and P. Schaaf, *Langmuir* 19, 9873 (2003).
56. T. J. Halthur, P. M. Claesson, and U. M. Elofsson, *J. Am. Chem. Soc.* 126, 17009 (2004).
57. C. Tedeschi, M. Polli, M. P. Fontana, and O. Pieroni, *Thin Solid Films* 284–285, 174 (1996).
58. S. Y. Yang and M. F. Rubner, *J. Am. Chem. Soc.* 124, 2100 (2002).
59. D. Lee, S. Y. Yang, R. E. Cohen, and M. F. Rubner, *Polym. Mater. Sci. Eng.* 90, 526 (2004).
60. D. M. DeLongchamp and P. T. Hammond, *Langmuir* 20, 5403 (2004).
61. V. Kozlovskaya, S. Ok, A. Sousa, M. Libera, and S. A. Sukhishvili, *Macromolecules* 36, 8590 (2003).
62. H. Zhang, Z. Wang, Y. Zhang, and X. Zhang, *Langmuir* 20, 9366 (2004).
63. J. D. Hong, K. Lowack, J. Schmitt, and G. Decher, *Prog. Colloid Polym. Sci.* 93, 98 (1993).
64. M. Sano, Y. Lvov, and T. Kunitake, *Annu. Rev. Mater. Sci.* 26, 153 (1996).
65. D. Yoo, S. S. Shiratori, and M. F. Rubner, *Macromolecules* 31, 4309 (1998).
66. J. J. Harris and M. L. Bruening, *Langmuir* 16, 2006 (2000).
67. J. D. Mendelsohn, C. J. Barrett, V. V. Chan, A. J. Pal, A. M. Mayes, and M. F. Rubner, *Langmuir* 16, 5017 (2000).
68. A. Fery, B. Scholer, T. Cassagneau, and F. Caruso, *Langmuir* 17, 3779 (2001).
69. J. Hiller, J. D. Mendelsohn, and M. F. Rubner, *Nat. Mater.* 1, 59 (2002).
70. S. E. Burke and C. J. Barrett, *Biomacromolecules* 4, 1773 (2003).
71. B. Y. Kim and M. L. Bruening, *Langmuir* 19, 94 (2003).
72. O. Mermut and C. Barrett, *J. Analyst* 126, 1861 (2001).
73. J. Q. Sun, T. Wu, F. Liu, Z. Q. Wang, X. Zhang, and J. C. Shen, *Langmuir* 16, 4620 (2000).
74. B. Schoeler, E. Poptoshev, and F. Caruso, *Macromolecules* 36, 5258 (2003).
75. N. G. Hoogveen, M. A. C. Stuart, G. J. Fleer, and M. R. Böhmer, *Langmuir* 12, 3675 (1996).
76. E. Kharlampieva and S. A. Sukhishvili, *Langmuir* 19, 1235 (2003).
77. S. T. Dubas and J. B. Schlenoff, *Macromolecules* 34, 3736 (2001).
78. G. B. Sukhorukov, A. A. Antipov, A. Voigt, E. Donath, and H. Möhwald, *Macromol. Rapid Commun.* 22, 44 (2001).
79. H. H. Rmaile, T. R. Farhat, and J. B. Schlenoff, *J. Phys. Chem. B* 107, 14401 (2003).
80. G. B. Sukhorukov, H. Möhwald, G. Decher, and Y. Lvov, *Thin Solid Films* 284, 220 (1996).
81. H. P. Zheng, I. Lee, M. F. Rubner, and P. T. Hammond, *Adv. Mater.* 14, 569 (2002).
82. S. K. Tripathy, J. Kumar, and H. S. Nalwa, Eds., *Handbook of Polyelectrolyte-based Thin Films for Electronic and Photonic Applications*, American Scientific Publishers, Stevenson Ranch, CA (2002), Vol. 1, p. 1.
83. H. H. Rmaile and J. B. Schlenoff, *J. Am. Chem. Soc.* 125, 6602 (2003).
84. M. J. McShane, J. Q. Brown, K. B. Guice, and Y. Lvov, *J. Nanosci. Nanotech.* 2, 411 (2002).
85. T. J. Halthur and U. M. Elofsson, *Langmuir* 20, 1739 (2004).
86. G. Sauerbrey, *Z. Physik* 155, 206 (1959).
87. N. Benkirane-Jessel, P. Schwinte, P. Falvey, R. Darcy, Y. Haikel, P. Schaaf, J. C. Voegel, and J. Ogier, *Adv. Funct. Mater.* 14, 174 (2004).
88. F. Boulmedais, V. Ball, P. Schwinte, B. Frisch, P. Schaaf, and J. C. Voegel, *Langmuir* 19, 440 (2003).
89. D. T. Haynie, S. Balkundi, N. Palath, K. Chakravarthula, and K. Dave, *Langmuir* 20, 4540 (2004).
90. K. S. Birdi, D. T. Vu, L. Moesby, K. B. Anderson, and D. Kristensen, *Surf. Coat. Technol.* 67, 183 (1994).
91. C. A. Nicolae, S. Cantin-Rivière, A. El Abed, and P. Peretti, *Langmuir* 13, 5507 (1997).
92. I. Fujiwara, M. Ohnishi, and J. Seto, *Langmuir* 8, 2219 (1992).
93. D. T. Haynie, N. Palath, Y. Liu, B. Li, and N. Pargaonkar, *Langmuir* 21, 1136 (2005).
94. M. Debrecezy, V. Ball, F. Boulmedais, B. Szalontai, J. C. Voegel, and P. Schaaf, *J. Phys. Chem. B* 107, 12734 (2003).
95. S. Zhang and A. Rich, *Proc. Natl. Acad. Sci. USA* 94, 23 (1997).
96. M. Müller, B. Kessler, and K. Lunkwitz, *J. Phys. Chem. B* 107, 8189 (2003).
97. N. J. Greenfield and G. D. Fasman, *Biochemistry* 8, 4108 (1969).
98. L. Zhang, B. Li, Z. L. Zhi, and D. T. Haynie, *Langmuir* 21, 5439 (2005).
99. G. Decher and J. B. Schlenoff, Eds., *Multilayer Thin Films: Sequential Assembly of Nanocomposite Materials*, Wiley-VCH, Weinheim (2002).
100. G. B. Sukhorukov, M. M. Montrel, A. I. Petrov, L. I. Shabarchina, and B. I. Sukhorukov, *Biosens. Bioelectron.* 11, 913 (1996).
101. M. M. Montrel, G. B. Sukhorukov, A. I. Petrov, L. I. Shabarchina, and B. I. Sukhorukov, *Sens. Actuators, B* 42, 225 (1997).
102. X. L. Hou, L. X. Wu, L. Sun, H. Zhang, B. Yang, and J. C. Shen, *Polym. Bull.* 47, 445 (2002).
103. Y. Okahata, T. Tsuruta, K. Ijio, and K. Ariga, *Thin Solid Films* 180, 65 (1989).
104. M. Sawodny, A. Schmidt, C. Urban, H. Ringsdorf, and W. Knoll, *Makromol. Chem. Macromol. Symp.* 46, 217 (1990).
105. B. Zheng, D. T. Haynie, H. Zhong, K. Sabnis, V. Surpuriya, N. Pargaonkar, G. Sharma, and K. Vistakula, *J. Biomater. Sci. Polym. Ed.* 16, 285 (2005).
106. J. Ruths, F. Essler, G. Decher, and H. Riegler, *Langmuir* 16, 8871 (2000).
107. R. Advincula, E. Aust, W. Meyer, and W. Knoll, *Langmuir* 12, 3536 (1996).
108. P. Bertrand, A. Jonas, A. Laschewsky, and R. Legras, *Macromol. Rapid Commun.* 21, 319 (2000).
109. C. Picart, J. Mutterer, L. Richert, Y. Luo, G. D. Prestwich, P. Schaaf, J. C. Voegel, and P. Laval, *Proc. Natl. Acad. Sci. USA* 99, 12531 (2002).

110. S. S. Shiratori and M. F. Rubner, *Macromolecules* 33, 4213 (2000).
111. K. Buscher, K. Graf, H. Ahrens, and C. A. Helm, *Langmuir* 18, 3585 (2002).
112. H. L. Tan, M. J. McMurdo, G. Pan, and P. G. van Patten, *Langmuir* 19, 9311 (2003).
113. M. Müller, *Biomacromolecules* 2, 262 (2001).
114. M. Müller, M. Brissova, T. Rieser, A. C. Powers, and K. Lunkwitz, *Mat. Sci. Eng. C* 8–9, 163 (1999).
115. X. Arys, A. Laschewsky, and A. M. Jonas, *Macromolecules* 34, 3318 (2001).
116. J. J. Harris, P. M. DeRose, and M. L. Bruening, *J. Am. Chem. Soc.* 121, 1978 (1999).
117. V. Kabanov and A. Zezin, *Pure Appl. Chem.* 56, 343 (1984).
118. V. Kabanov, *Polym. Sci.* 36, 143 (1994).
119. J. L. Stair, J. J. Harris, and M. L. Bruening, *Chem. Mater.* 13, 2641 (2001).
120. M. K. Park, C. J. Xia, R. C. Advincula, P. Schutz, and F. Caruso, *Langmuir* 17, 7670 (2001).
121. E. Brynda and M. Houska, *J. Colloid Interface Sci.* 183, 18 (1996).
122. W. Tong, C. Gao, and H. Möhwald, *Chem. Mater.* 17, 4610 (2005).
123. X. Zhang, J. Sun, and J. Shen, in *Multilayer Thin Films: Sequential Assembly of Nanocomposite Materials*, G. Decher and J. B. Schlenoff, Eds., Wiley-VCH, Weinheim (2002), p. 301.
124. H. Kawaguchi, *Prog. Polym. Sci.* 25, 1171 (2000).
125. M. Morikawa, M. Yoshihara, T. Endo, and N. Kimizuka, *Chem. Eur. J.* 11, 1574 (2005).
126. T. Kidchob, S. Kimura, and Y. Imanishi, *J. Appl. Polym. Sci.* 63, 453 (1997).
127. S. B. Wang, F. H. Xu, H. S. He, and L. J. Weng, *Macromol. Biosci.* 5, 408 (2005).
128. E. Donath, G. B. Sukhorukov, F. Caruso, S. Davis, and H. Möhwald, *Angew. Chem., Int. Ed.* 37, 2201 (1998).
129. Y. Lvov, A. A. Antipov, A. Mamedov, H. Möhwald, and G. B. Sukhorukov, *Nano. Lett.* 1, 125 (2001).
130. N. P. E. Vermeulen and J. M. te. Koppele, in *Drug Stereochemistry: Analytical Methods and Pharmacology*, 2nd ed., W. I. Wainer, Ed., Marcel Dekker, New York (1993), p. 245.
131. B. Li and D. T. Haynie, in *Encyclopedia of Chem. Proc.*, Sungyu Lee, Ed., Taylor & Francis, New York (2005), Vol. 1, p. 449.
132. M. W. Kamande, X. Zhu, C. Kapnissi-Christodoulou, and I. M. Warner, *Anal. Chem.* 76, 6681 (2004).
133. A. M. Hollman and D. Bhattacharyya, *Langmuir* 20, 5418 (2004).
134. S. Berwald and J. Meier-Haack, in *Handbook of Polyelectrolytes and Their Applications*, S. K. Tripathy, J. Kumar, and H. S. Nalwa, Eds., American Scientific Publishers, Stevenson Ranch, CA (2002), Vol. 1, p. 99.
135. B. Tieke, in *Handbook of Polyelectrolytes and Their Applications*, S. K. Tripathy, J. Kumar, and H. S. Nalwa, Eds., American Scientific Publishers, Stevenson Ranch, CA (2002), Vol. 3, p. 115.
136. J. Dai, A. M. Balachandra, J. I. Lee, and M. L. Bruening, *Macromolecules* 35, 3164 (2002).
137. W. Jin, A. Toutianoush, and B. Tieke, *Langmuir* 19, 2550 (2003).
138. B. W. Stanton, J. J. Harris, M. D. Miller, and M. L. Bruening, *Langmuir* 19, 7038 (2003).
139. T. C. McDevitt, K. E. Nelson, and P. S. Stayton, *Biotechnol. Prog.* 15, 391 (1999).

Li B. Polypeptide multilayer films and microcapsules. Soft Nanomaterials, Ed. Nalwa HS.  
Vol. 2, 123-150, 2009. American Scientific Publishers, Stevenson Ranch, California.